because Izumo is not localized on plasma membrane of fresh spermatozoa but is hidden under plasma membrane and accessible after the acrosome reaction, as occurs with CD46 on mouse sperm[6].

To address the physiological role of Izumo *in vivo* we generated *Izumo*-deficient mice by homologous recombination. An *Izumo*-targeting construct was designed to replace exons 2–10 with a

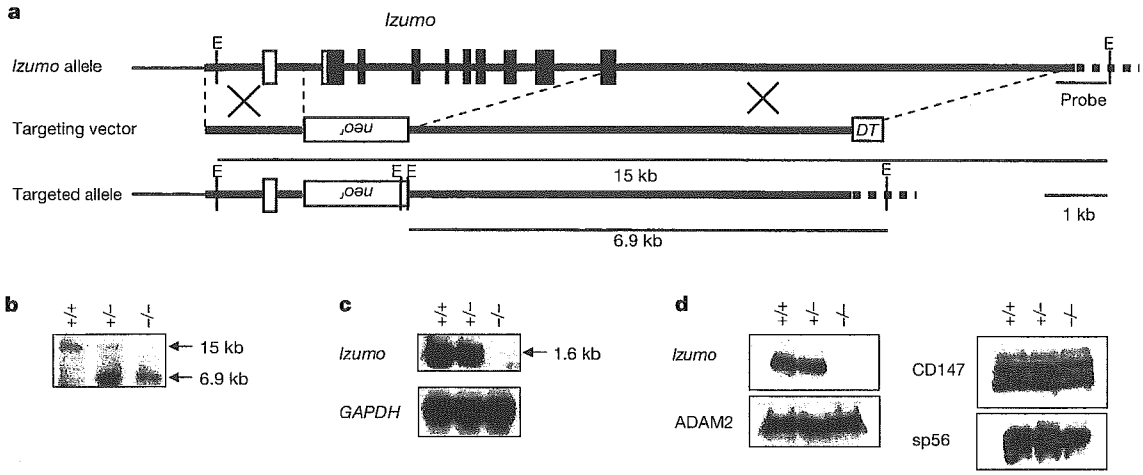

Figure 2 Targeted disruption of *Izumo* gene. **a**, Complete structures of the wild-type mouse *Izumo* allele, targeting vector and mutant allele. Exons and introns are represented by vertical bars and horizontal lines, respectively. A neomycin-resistance gene driven by a phosphoglycerine kinase (PGK) promoter (*neo*^{r}) and a diphtheria toxin A chain driven by a MC1 promoter (DT) are shown as white boxes. **b**, Southern blot genotyping confirmed gene disruption. Hybridization of the 3′ external probe with *Eco*RI-digested genomic DNA yielded 15-kb (wild type) and 6.9-kb (mutant) bands. **c**, Northern blot of total testis RNA (20 μg) from wild-type (+/+), heterozygous (+/−) and homozygous (−/−) mice. GAPDH is shown as a loading control. **d**, By western blotting, Izumo protein was undetectable in mutant mice. Various sperm proteins (30 μg per lane) were detectable by western blotting in sperm from *Izumo* $^{-/-}$ mice as well as wild-type and heterozygous animals. From the top, Izumo, ADAM2 (9D2.2; Chemicon), CD147 (Santa Cruz) and sp56 (7C5; QED Biologicals) are shown.

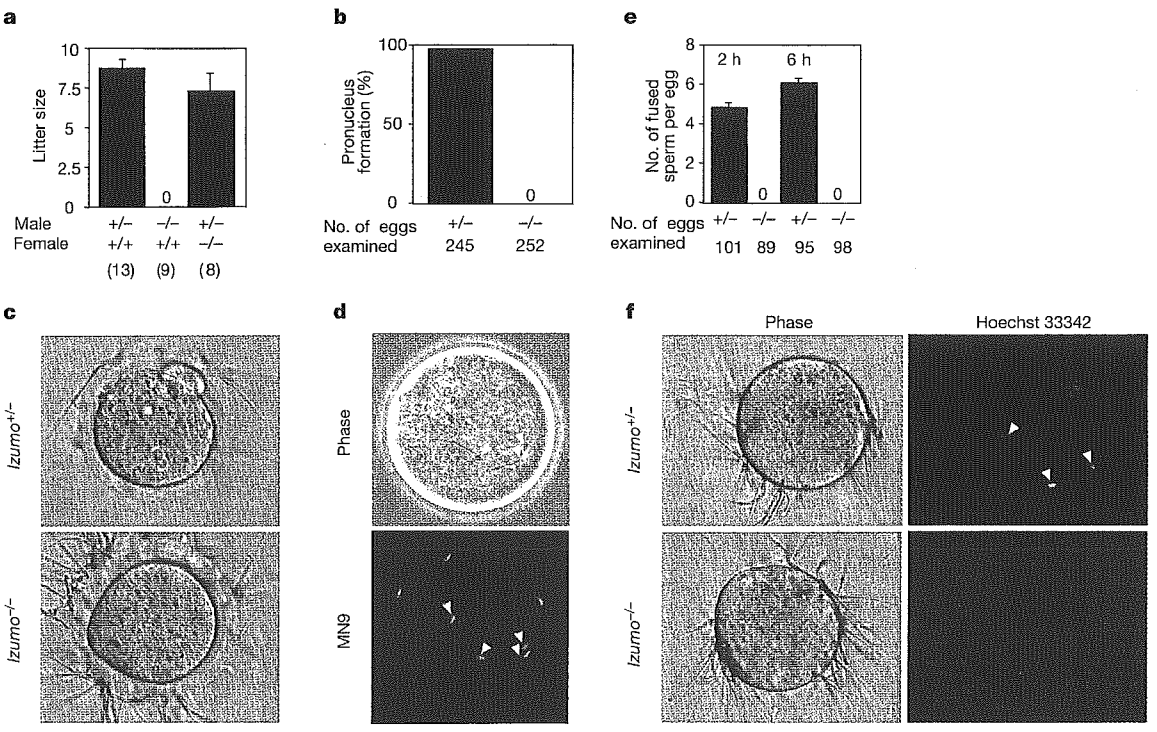

Figure 3 Male infertility caused by *Izumo* disruption. **a**, Fecundity of *Izumo* $^{+/-}$ and *Izumo* $^{-/-}$ males and *Izumo* $^{-/-}$ females. The numbers in parentheses indicate the numbers of mating pairs. **b**, **c**, *In vitro* fertilization of sperm from *Izumo* $^{+/-}$ and *Izumo* $^{-/-}$ mice. Unlike *Izumo* $^{+/-}$, the eggs inseminated with *Izumo* $^{-/-}$ sperm had many sperm on their zona pellucida, owing to the failure of sperm–egg fusion that probably leads to the absence of zona-reaction to lessen the sperm-binding ability of the zona pellucida. The error bars in **b** are not visible ($n = 5$). **d**, Upper panel, accumulation of many sperm in the perivitelline space of the eggs recovered from the females mated with *Izumo* $^{-/-}$ males. Lower panel, sperm in perivitelline space labelled with acrosome-reacted, sperm-specific monoclonal antibody MN9 (ref. 15). **e**, Average numbers of fused sperm observed 2 and 6 h after insemination ($n = 5$). **f**, Fused sperm stained by Hoechst 33342 preloaded into the egg. The arrowheads show the fused sperm. Errors bars in **a** and **e** are s.e.m.

neomycin-resistant gene (*neo*^{r}) (Fig. 2a). Both the targeting event in D3 embryonic stem cells and the germline transmission of targeted genes were confirmed by Southern blot analysis (Fig. 2b). In the homozygous mutant mice, the full-length (1.6-kilobase (kb)) messenger RNA (Fig. 2c) and the Izumo protein (Fig. 2d) were not detected. Because the disruption of a gene can cause a concomitant increase or decrease in some related genes[7], we examined ADAM2 (ref. 8), CD147 (ref. 9) and sp56 (ref. 10), which were reported to be involved in sperm–egg interactions. We could not find a significant change in these protein levels in sperm after the deletion of *Izumo* gene (Fig. 2d).

Intercrosses between heterozygous F_1 mice yielded offspring that segregated in a mendelian distribution: 43 wild-type, 92 heterozygous and 47 homozygous mutant weaning pups. *Izumo*$^{-/-}$ mutant mice were healthy and showed no overt developmental abnormalities. *Izumo*$^{-/-}$ females demonstrated normal fecundity. *Izumo*$^{+/-}$ males also showed normal fertilizing ability (Fig. 3a). However, *Izumo*$^{-/-}$ males were sterile despite normal mating behaviour and ejaculation, with normal vaginal plug formations. After observation of 28 plugs, nine pairs of *Izumo*$^{-/-}$ male and wild-type females were kept for another 4 months but no pregnancies were observed (Fig. 3a). In at least four different cases of gene knockouts that resulted in male sterility attributed to impaired zona-binding ability, the sperm also failed to migrate into the oviduct[7,8,11,12]. However, disruption of *Izumo* did not cause any defect in sperm migration into the oviduct (data not shown, and there was no reduction of sperm motility in *Izumo*$^{-/-}$ sperm; motility was measured 120 min after incubation by computer-aided sperm analysis (CASA; mean ± s.e.m. = 81.7 ± 7.7% in *Izumo*$^{+/-}$ sperm and 77 ± 8.9% in *Izumo*$^{-/-}$ sperm)). The sterile nature of *Izumo*$^{-/-}$ sperm was shown in the *in vitro* fertilization system (Fig. 3b, c, and Supplementary Movie 1). The impaired fertilization step undoubtedly followed zona penetration because sperm penetrated the zona pellucida and accumulated in the perivitelline space of the eggs (Fig. 3d).

Syngamy can be considered to occur to two stages: binding of the sperm plasma membrane to that of the egg, and actual membrane fusion. *Izumo*$^{-/-}$ sperm were capable of binding to the plasma membranes of eggs whose zona pellucida had been mechanically removed[13](Fig. 3e, f). In this system, the *Izumo*$^{+/-}$ sperm incubated for 2 and 6 h fused to eggs in approximate ratios of 4.5 and 6 sperm per egg, respectively, but no *Izumo*$^{-/-}$ sperm fused with eggs.

Sperm cannot fuse with eggs unless the former have undergone the acrosome reaction[14]. To verify the acrosomal status of *Izumo*$^{-/-}$ sperm, we stained the sperm accumulated in perivitelline spaces with the MN9 monoclonal antibody, which immunoreacts only to the equatorial segment of acrosome-reacted sperm[15]. The staining indicated that the *Izumo*$^{-/-}$ sperm had undergone the acrosome reaction (Fig. 3d) but failed to fuse with eggs.

Because no offspring were fathered by *Izumo*$^{-/-}$ male mice, it was unclear whether the defect was limited to fusion or extended to later developmental stages. To address this question, we used intracytoplasmic sperm injection (ICSI) to insert *Izumo*$^{-/-}$ sperm directly into the cytoplasm of wild-type eggs and bypass the fusion step[16]. Eggs injected with *Izumo*$^{-/-}$ sperm were successfully activated and the fertilized eggs were transplanted into the oviducts of pseudopregnant females. The eggs implanted normally and the resulting embryos developed appropriately to term with rates similar to those of heterozygous mice (Table 1).

Sperm–egg fusion is known to be less species-specific than sperm–zona interaction. For example, human sperm cannot penetrate the hamster zona pellucida but they can fuse with zona-free hamster eggs, and this system (zona-free hamster-egg sperm penetration test) has been used for the assessment of human sperm fertility[17]. We first examined the contribution of mouse Izumo in a zona-free hamster-egg sperm penetration assay. As indicated in Fig. 4a, the mouse Izumo was essential not only in the homologous fusion system but also for heterologous fusion with hamster eggs. Similarly, when the anti-human Izumo polyclonal antibody was added to the incubation mixture, no fusion was observed, whereas the sperm treated with control IgG fused with eggs at an average of 5.9 ± 0.7 sperm per egg. The total numbers of eggs observed were 23 and 29, respectively (n=3). These results indicated that human Izumo is involved in the fertilization process in human sperm (Fig. 4b). However, further investigation will be required to explain the function of Izumo in human fertilization because adding the antibody caused inhibition of human sperm binding to the egg plasma membrane in the heterologous sperm–egg fusion system.

The phenotypes of gene knockout mice are not always related to the disrupted genes but are sometimes caused by disruption of a neighbouring gene[18]. To examine whether the phenotype was directly derived from the lack of Izumo on sperm, we performed a rescue experiment by crossing *Izumo*$^{-/-}$ mice with transgenic mouse

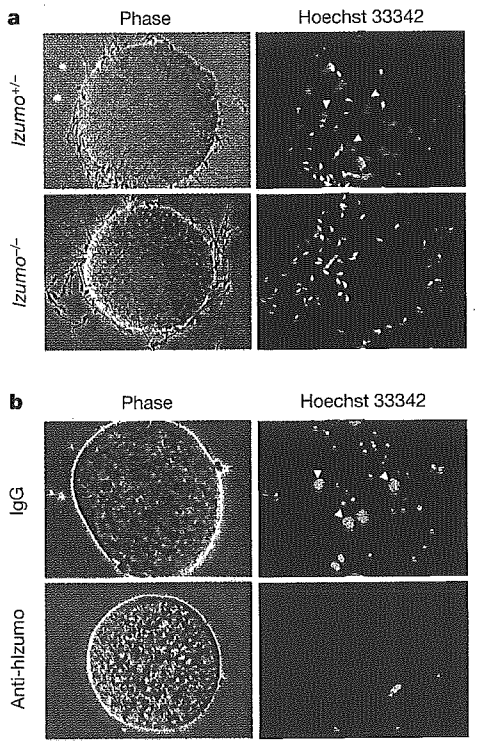

Figure 4 Involvement of Izumo in a xeno-species fusion system. **a**, At 6 h after the insemination of zona-free hamster eggs with *Izumo*$^{+/-}$ and *Izumo*$^{-/-}$ mouse sperm, sperm heads were stained by adding Hoechst 33342 to the medium. The sperm–egg binding was strong enough to resist repeated pipetting. **b**, Human sperm were also added with 25 μg ml^{-1} anti-human Izumo (anti-hIzumo) or control IgG to zona-free hamster eggs (n=3). No fusion was observed in the presence of anti-Izumo antibody. Arrowheads indicate the swelling sperm head after staining with Hoechst 33342. The eggs were pressed under a coverslip to bring many sperm into focus.

Table 1 **Development of eggs after ICSI with *Izumo*$^{-/-}$ sperm**

Sperm	No. of eggs used	No. of eggs surviving after ICSI	No. of eggs developing to two-cell stage	No. of pups born
Izumo$^{-/-}$	95	59	42 (71%)*	12 (29%)†
Izumo$^{+/-}$	85	54	43 (80%)	6 (14%)

*Percentages are based on numbers of eggs surviving after ICSI.
†All offspring from *Izumo*$^{-/-}$ sperm were confirmed to possess the *Izumo*-null allele.

lines generated to express Izumo by using the testis-specific calmegin promoter[12]. The sterile phenotype was rescued with the transgenically expressed Izumo on mouse sperm (Supplementary Fig. 1).

In the search for sperm surface proteins that function in sperm–egg plasma-membrane binding and fusion, various candidates such as DE[19], CD46 (ref. 20), equatorin[15], Sperad[21] and SAMP32 (ref. 22) have been reported. ADAM family proteins are given the most attention for their possession of a putative fusion peptide (ADAM1) and disintegrin domain (ADAM2 and ADAM3)[23]. None of the mice possessing disrupted ADAM1a, ADAM2 and ADAM3 show a significant defect in the ability to fuse with eggs[7,8,24], but do show an impairment of sperm–zona binding ability. Similarly, CD46 disruption does not diminish fusion[6]. In contrast, CD9 on the egg surface is essential for the fusing ability of eggs[2–4] and some indications for the involvement of the binding of integrins to CD9 are postulated in reference to sperm–egg fusion. However, the disruptions of the most probable candidate integrins α6 and β1 cause no major influence on the fusing ability of eggs[25]. Thus, for several years, postulated fertilization mechanisms were repeatedly changed as a result of gene disruption experiments. This suggests that the essential nature of the candidate gene must be judged after observing the phenotype of the gene-disrupted mice. In this context, Izumo is the first sperm membrane protein shown to be essential for fusion. It is not yet known whether sperm Izumo interacts with egg CD9, as occurs with placental IgSF protein PSG17 (ref. 26); neither do we know why the localization of Izumo after acrosome reaction is not limited to the equatorial segment where fusion initially takes place. All we can say now is that continued study of this protein's function will undoubtedly lead to a fuller understanding of the cell–cell fusion process in fertilization and perhaps in other somatic systems such as muscle cells or trophoblasts.

The finding not only provides insight into the enigmatic fusion mechanism but also promises benefits in the clinical treatment of infertility and the potential development of new contraceptive strategies. □

Methods

Cloning of *Izumo*

Izumo amino acid sequences were determined by combining two-dimensional gel electrophoresis and LC–MS/MS. Some peptide sequences (Fig. 1a, shown in red) were analysed and identified as members of an immunoglobulin superfamily protein (NCBI accession number XM_133424) whose function was not clarified. To confirm the DNA sequence we used RT–PCR to amplify Izumo from mouse testis RNA as a template with primers derived from this sequence. The polyclonal antibodies against mouse and human Izumo were produced by immunizing an Izumo-expressing RK13 cell line into rabbits[27].

Generation of *Izumo* knockout mice

A targeting vector was constructed with the use of pMulti-ND 1.0 containing the Neo-resistance gene (*neo*^{r}) as a positive selection marker and diphtheria toxin A chain (DT) as a negative selection marker (provided by J. Takeda and T. Ijiri). A 1.7-kb *Asc*I–*Pac*I fragment and a 6.7-kb *Cla*I–*Xho*I fragment were inserted as a short and long arm, respectively. Embryonic stem cells derived from 129/Sv (D3) were electroporated with *Pme*I-digested linearized DNA. Of 385 G418-resistant clones, four had undergone homologous recombination correctly. Three targeted cell lines were injected into C57BL/6 blastocysts, resulting in the birth of male chimaeric mice. These mice were then crossed with C57BL/6 to obtain heterozygous mutants. Mice used in the study were the offspring of crosses between F_1 and/or F_2 generations.

In vitro fertilization

Mouse sperm were collected from cauda epididymides and capacitated *in vitro* for 2 h in a 200-μl drop of TYH medium[28] covered with paraffin oil. Wild-type female mice (more than 8 weeks old) were superovulated by the injection of 5 U of human chorionic gonadotropin (hCG) 48 h after a 5-U injection of pregnant mare serum gonadotropin. The eggs were collected from the oviduct 14 h after the hCG injection. Eggs were placed in a 200-μl drop of TYH medium. These eggs were incubated with 2×10^5 *Izumo*$^{+/-}$ or *Izumo*$^{-/-}$ sperm per ml incubated for 2 h at 37 °C in 5% CO_2, and unbound sperm were washed away. Eggs were observed 6 h after insemination for the formation of pronuclei under a Hoffman modulation contrast microscope.

Zona-free-egg sperm penetration assay

After being freed from cumulus cells with 0.01% (w/v) hyaluronidase, the zona pellucida was removed from mouse or hamster eggs with a piezo-manipulator as described previously[13]. Fusion assessment was performed in two different ways. In the first method, zona-free mouse oocytes were preloaded with Hoechst 33342 by incubating them with the dye (1 μg ml^{-1}) in TYH for 10 min and washing them before addition of the sperm. After 30 min of incubation, the eggs were observed under a fluorescence microscope (excitation with ultraviolet) after fixing with 0.25% glutaraldehyde. This procedure enabled the staining of only fused sperm nuclei by transferring the dye into sperm after membrane fusion as in Fig. 3. Alternatively, in the second method the zona-free hamster eggs were incubated for 6 h with sperm without preloading of the dye. By this time, enlarged sperm heads could be seen when fusion occurred. The eggs with sperm were incubated in 1 μg ml^{-1} Hoechst 33342 for 10 min to ensure that all bound (original sperm head shape) and fused (enlarged round shape) sperm would be stained with the dye, as in Fig. 4. In all experiments the human sperm were collected from liquefied semen by the swim-up method and incubated for 6 h before addition to eggs. We used BWW medium[29] containing 35 mg ml^{-1} human serum albumin (HSA) for the human sperm experiment.

Received 12 October 2004; accepted 17 January 2005; doi:10.1038/nature03362.

1. Stein, K. K., Primakoff, P. & Myles, D. Sperm–egg fusion: events at the plasma membrane. *J. Cell Sci.* **117**, 6269–6274 (2004).
2. Miyado, K. *et al.* Requirement of CD9 on the egg plasma membrane for fertilization. *Science* **287**, 321–324 (2000).
3. Le Naour, F., Rubinstein, E., Jasmin, C., Prenant, M. & Boucheix, C. Severely reduced female fertility in CD9-deficient mice. *Science* **287**, 319–321 (2000).
4. Kaji, K. *et al.* The gamete fusion process is defective in eggs of CD9-deficient mice. *Nature Genet.* **24**, 279–282 (2000).
5. Okabe, M. *et al.* Capacitation-related changes in antigen distribution on mouse sperm heads and its relation to fertilization rate *in vitro*. *J. Reprod. Immunol.* **11**, 91–100 (1987).
6. Inoue, N. *et al.* Disruption of mouse CD46 causes an accelerated spontaneous acrosome reaction in sperm. *Mol. Cell. Biol.* **23**, 2614–2622 (2003).
7. Nishimura, H., Kim, E., Nakanishi, T. & Baba, T. Possible function of the ADAM1a/ADAM2 fertilin complex in the appearance of ADAM3 on the sperm surface. *J. Biol. Chem.* **279**, 34957–34962 (2004).
8. Cho, C. *et al.* Fertilization defects in sperm from mice lacking fertilin beta. *Science* **281**, 1857–1859 (1998).
9. Saxena, D. K., Oh-Oka, T., Kadomatsu, K., Muramatsu, T. & Toshimori, K. Behaviour of a sperm surface transmembrane glycoprotein basigin during epididymal maturation and its role in fertilization in mice. *Reproduction* **123**, 435–444 (2002).
10. Bookbinder, L. H., Cheng, A. & Bleil, J. D. Tissue- and species-specific expression of sp56, a mouse sperm fertilization protein. *Science* **269**, 86–89 (1995).
11. Hagaman, J. R. *et al.* Angiotensin-converting enzyme and male fertility. *Proc. Natl Acad. Sci. USA* **95**, 2552–2557 (1998).
12. Ikawa, M. *et al.* Calmegin is required for fertilin alpha/beta heterodimerization and sperm fertility. *Dev. Biol.* **240**, 254–261 (2001).
13. Yamagata, K. *et al.* Sperm from the calmegin-deficient mouse have normal abilities for binding and fusion to the egg plasma membrane. *Dev. Biol.* **250**, 348–357 (2002).
14. Yanagimachi, R. *Mammalian Fertilization* (eds Knobil, E & Neill, J. D.) (Raven, New York, 1994).
15. Manandhar, G. & Toshimori, K. Exposure of sperm head equatorin after acrosome reaction and its fate after fertilization in mice. *Biol. Reprod.* **65**, 1425–1436 (2001).
16. Kimura, Y. & Yanagimachi, R. Intracytoplasmic sperm injection in the mouse. *Biol. Reprod.* **52**, 709–720 (1995).
17. Yanagimachi, R., Yanagimachi, H. & Rogers, B. J. The use of zona-free animal ova as a test-system for the assessment of the fertilizing capacity of human spermatozoa. *Biol. Reprod.* **15**, 471–476 (1976).
18. Olson, E. N., Arnold, H. H., Rigby, P. W. & Wold, B. J. Know your neighbors: three phenotypes in null mutants of the myogenic bHLH gene MRF4. *Cell* **85**, 1–4 (1996).
19. Rochwerger, L., Cohen, D. J. & Cuasnicu, P. S. Mammalian sperm–egg fusion: the rat egg has complementary sites for a sperm protein that mediates gamete fusion. *Dev. Biol.* **153**, 83–90 (1992).
20. Anderson, D. J., Abbott, A. F. & Jack, R. M. The role of complement component C3b and its receptors in sperm–oocyte interaction. *Proc. Natl Acad. Sci. USA* **90**, 10051–10055 (1993).
21. Ilayperuma, I. Identification of the 48-kDa G11 protein from guinea pig testes as sperad. *J. Exp. Zool.* **293**, 617–623 (2002).
22. Hao, Z. *et al.* SAMP32, a testis-specific, isoantigenic sperm acrosomal membrane-associated protein. *Biol. Reprod.* **66**, 735–744 (2002).
23. Blobel, C. P. *et al.* A potential fusion peptide and an integrin ligand domain in a protein active in sperm–egg fusion. *Nature* **356**, 248–252 (1992).
24. Nishimura, H., Cho, C., Branciforte, D. R., Myles, D. G. & Primakoff, P. Analysis of loss of adhesive function in sperm lacking cyritestin or fertilin beta. *Dev. Biol.* **233**, 204–213 (2001).
25. He, Z. Y. *et al.* None of the integrins known to be present on the mouse egg or to be ADAM receptors are essential for sperm–egg binding and fusion. *Dev. Biol.* **254**, 226–237 (2003).
26. Ellerman, D. A., Ha, C., Primakoff, P., Myles, D. G. & Dveksler, G. S. Direct binding of the ligand PSG17 to CD9 requires a CD9 site essential for sperm–egg fusion. *Mol. Biol. Cell* **14**, 5098–5103 (2003).
27. Inoue, N. *et al.* A novel chicken membrane-associated complement regulatory protein: molecular cloning and functional characterization. *J. Immunol.* **166**, 424–431 (2001).
28. Toyoda, Y., Yokoyama, M. & Hoshi, T. Studies on the fertilization of mouse egg *in vitro*. *Jpn. J. Anim. Reprod.* **16**, 147–151 (1971).
29. Overstreet, J. W., Yanagimachi, R., Katz, D. F., Hayashi, K. & Hanson, F. W. Penetration of human spermatozoa into the human zona pellucida and the zona-free hamster egg: a study of fertile donors and infertile patients. *Fertil. Steril.* **33**, 534–542 (1980).
30. Nakanishi, T. *et al.* Real-time observation of acrosomal dispersal from mouse sperm using GFP as a marker protein. *FEBS Lett.* **449**, 277–283 (1999).
31. Okabe, M. *et al.* A human sperm antigen possibly involved in binding and/or fusion with zona-free hamster eggs. *Fertil. Steril.* **54**, 1121–1126 (1990).

Supplementary Information accompanies the paper on **www.nature.com/nature**.

Acknowledgements We thank K. Toshimori for providing anti-MN9 antibody; K. Yamagata for discussions; G. L. Gerton and S. Moss for critically reviewing the draft; and Y. Maruyama, A. Kawai and Y. Koreeda for technical assistance with gene disruption. This work was supported by grant-in-aid for Scientific Research and the 21st Century COE program from the Ministry of Education, Culture, Sports, Science, and Technology of Japan.

Competing interests statement The authors declare that they have no competing financial interests.

Correspondence and requests for materials should be addressed to M.O. (e-mail: okabe@gen-info.osaka-u.ac.jp). Sequences have been deposited with GenBank under accession numbers AB195681 for mouse *Izumo*, AB195682 for human *Izumo* and AB195683 for rat *Izumo*.

Genomic imprinting of XX spermatogonia and XX oocytes recovered from XX↔XY chimeric testes

Ayako Isotani[†‡], Tomoko Nakanishi[†§], Shin Kobayashi[†¶‖], Jiyoung Lee[¶‖††], Shinichiro Chuma[‡‡], Norio Nakatsuji[‡‡], Fumitoshi Ishino[¶‖††], and Masaru Okabe[†‡§§]

[†]Genome Information Research Center and [‡]Graduate School of Pharmaceutical Sciences, Osaka University, 3-1 Yamadaoka, Suita, Osaka 565-0871, Japan; [¶]Gene Research Center, Tokyo Institute of Technology, Kanagawa 226-8501, Japan; [‖]Core Research for Evolutional Science and Technology, Japan Science and Technology Corporation, Chuou-ku, Tokyo 113-0027, Japan; and [‡‡]Department of Development and Differentiation, Institute for Frontier Medical Sciences, Kyoto University, 53 Kawahara-cho Shogoin, Sakyo-ku, Kyoto 606-8507, Japan

Edited by Ryuzo Yanagimachi, University of Hawaii, Honolulu, HI, and approved February 1, 2005 (received for review September 13, 2004)

We produced XX↔XY chimeras by using embryos whose X chromosomes were tagged with EGFP (X*), making the fluorescent green female (XX*) germ cells easily distinguishable from their nonfluorescent male (XY) counterparts. Taking advantage of tagging with EGFP, the XX* "prospermatogonia" were isolated from the testes, and the status of their genomic imprinting was examined. It was shown that these XX cells underwent a paternal imprinting, despite their chromosomal constitution. As previously indicated in sex-reversal XXsxr testes, we also found a few green XX* germ cells developed as "eggs" within the seminiferous tubules of XX*↔XY chimeric testes. These cells were indistinguishable from XX* prospermatogonia at birth but resumed oogenesis in a testicular environment. The biological nature of the "testicular eggs" was examined by recovering the eggs from chimeric testes. The testicular eggs not only formed an egg-specific structure, the zona pellucida, but also were able to fuse with sperm. The collected testicular eggs were indicated to undergo maternal imprinting, despite the testicular environment. The genomic imprinting did not always follow the environmental conditions of where the germ cells resided; rather, it was defined by the sex that was chosen by the germ cells at early embryonic stage.

sex differentiation | XX prospermatogonia | EGFP | XX↔XY chimera | genomic imprinting

To reproduce, mammals must develop as either males or females. In general, sex is determined by the sex chromosomal complement at the time of fertilization; i.e., the presence of a Y chromosome confers "maleness." However, the mammalian gonads are reported to arise as a bipotential primordium with the plasticity to develop into an ovary or a testis (1). In the process of testicular differentiation, Sertoli cells that express *Sry* are considered to play an important role. For example, if *Sry* expression were delayed and/or diminished, the resultant animals would show sex reversal (2–4). Conversely, if exogenously integrated *Sry* is expressed in XX mouse gonads, they develop into male testes (5).

Germ cells also have the plasticity to develop as either oogonia or "prospermatogonia." If XX primordial germ cells are sequestered in the testicular cord, they are reported to develop as prospermatogonia from their arrested mitosis and prominent nucleoli structures (6–8).

Although mouse primordial germ cells are dimorphic, the fate of "XX prospermatogonia" in the testis after birth is different from that of XY prospermatogonia. All XX prospermatogonia die within the first few days postpartum (dpp), whereas the XY prospermatogonia proliferate and begin spermatogenesis (7, 9, 10). This difference might be due to the absence of Y-linked spermatogenesis genes in XX cells (11, 12). However, it is known that Y chromosomes bearing XXY spermatogonia also disappear from the testis (13, 14). Thus, a precise mechanism of disappearance of XX prospermatogonia before differentiation is yet to be elucidated.

A useful indicator for sex differentiation in germ-line cells could be the establishment of genomic imprinting during gametogenesis (15). After removal of the imprinting during the primordial germ-cell stage, new imprints are imposed in prospermatogonia before they enter meiosis (16, 17). In contrast, nongrowing primary oocytes, such as those in newborn mice, have not established differential methylation in several differentially methylated regions (DMRs). In oocytes, new imprints are imposed later at different stages of oogenesis for different genes, from very early to the antral follicle stage (18, 19).

By tagging the sex chromosomes with a ubiquitously expressed EGFP transgene (20, 21), we can determine the sex of the preimplantation embryos noninvasively (22). Moreover, if the EGFP-tagged (hereafter designated with an *) embryos then are used to make chimeras, we can visualize the contribution of XX* cells by green fluorescence.

XX somatic and germinal lineages undergo random X-chromosome inactivation together; during gastrulation (23), the inactive X chromosome in "XX germ cells" then undergoes reactivation around the time of entry into the genital ridges, whether the embryo is female (24) or male (25). These findings have been confirmed by Tam and colleagues (26, 27) and extended by studies on *Xist* expression. Therefore, it may not be possible to trace all of the XX* cells in somatic tissue because one of the X chromosomes is silenced by X inactivation (28), but germ-line cells can be traced because X inactivation does not take place in germ-line cells in the genital ridge (26, 27). One of the advantages of using EGFP-tagged cells is the easy identification of cells, even when they are sparsely distributed (29). In the present study, we recovered the XX* germ-line cells from the XX*↔XY chimeric testes to examine the elasticity of germ-cell sex in molecular bases.

Materials and Methods

Animals. The handling and surgical manipulation of all experimental animals were carried out according to the guidelines of the Committee on the Use of Live Animals in Teaching and Research of Osaka University. We produced six mouse lines whose X chromosomes contain a transgene consisting of EGFP expressed from a CAG promoter (combination of a β-actin promoter and a human cytomegalovirus enhancer) (20). For the experiments presented in this report, we used two transgenic lines of X-linked EGFP [B6C3F1 TgN (act EGFP) Osb CX-50

This paper was submitted directly (Track II) to the PNAS office.

Abbreviations: dpp, days postpartum; dpc, days postcoitum; DMR, differentially methylated region; SCP3, synaptonemal complex protein 3.

[§]Present address: Institute of Applied Biochemistry, University of Tsukuba, Tsukuba Science City, Ibaraki 305-8572, Japan.

[††]Present address: Department of Epigenetics, Medical Research Institute, Tokyo Medical and Dental University, 2-3-10 Kanda-Surugadai, Chiyoda-ku, Tokyo 101-0062, Japan.

[§§]To whom correspondence should be addressed. E-mail: okabe@gen-info.osaka-u.ac.jp.

(no. 50) and B6C3F1 TgN (act EGFP) Osb CX-139 (no. 139) (20)]. When we used the former line, we detected the contribution of all cells possessing XX* chromosomes, because the EGFP fluorescence is equally bright in germ-line and somatic cells. With the latter line, the germ cells could be separated by FACS, based on the difference of EGFP fluorescence in germline (bright) and somatic (faint) cells.

Production of XX*↔XY Chimera. Aggregation chimeras were produced as described in ref. 30. Briefly, superovulated (B6C3F1) females (XX) were mated with males whose X chromosome was tagged with EGFP (X*Y). Two- or four-cell-stage embryos were collected and placed in K^+-modified simplex optimized medium (31), covered with mineral oil, and incubated overnight at 37°C in 95% air/5% CO_2. Male (EGFP-negative) and female (EGFP-positive) embryos were separated at the eight-cell and early morula stage by using a fluorescent microscope (IX-70 with U-MWIBA filter set, Olympus, Melville, NY) micromanipulator. After removing the zona pellucida with acidic Tyrode's solution (Sigma), male and female embryos were paired in aggregation wells and incubated overnight at 37°C in 95% air/5% CO_2. XX*↔XY chimeric embryos were then transferred into the uterus of 2.5-days postcoitum (dpc) pseudopregnant recipients.

Preparation of Testicular and Ovarian Germ Cells. Newborn (0-dpp) germ cells were prepared (32). The testes (20–30) of newborn males and XX*↔XY chimera males were incubated in 1 mg/ml collagenase (type I, Sigma) in DMEM buffered with 20 mM Hepes (pH 7.4) at 32°C for 15 min. After pipeting to separate the seminiferous tubules, the tubules were washed in PBS (−) and incubated with 0.25% trypsin in PBS (−) supplemented with 1 mM EDTA at 32°C for 10 min. Single cells were obtained by pipetting, filtering through a nylon mesh, and centrifuging at 700 × *g* for 5 min at 4°C. Ovarian cells were prepared by incubating ovaries at 37°C for 15 min after mincing them in 1 mM EDTA in PBS (−) followed by pipetting. The freed cells were filtered through nylon mesh, centrifuged, and resuspended in Hepes-buffered saline solution containing 0.1% BSA.

Both male and female cells were sorted by using a FACSVantage cell sorter (Becton Dickinson). "Testicular eggs" were recovered from chimeric male testes at 1–3 weeks of age. After removing the tunica albuginea, the seminiferous tubules were spread out by gently pulling a part of the tubules under a fluorescent microscope. The tubule sections containing testicular eggs were cut with Noyes spring scissors. While holding one end with Dumont no. 5 tweezers, the contents of the tubes were squeezed out by gently pinching and sliding with supplemental tweezers. The testicular eggs were then collected by using a finely drawn pipette.

For further details about experimental materials and methods, see *Supporting Materials and Methods*, which is published as supporting information on the PNAS web site.

Results

Production of XX*↔XY Chimera by Using EGFP-Tagged X Chromosomes and XX* Derived Cells in Testes. Males with an X-linked EGFP (X*) transgene (20) were bred with wild-type females. Eggs fertilized by X* sperm (female eggs) showed EGFP fluorescence at about the eight-cell stage. After separating male and female embryos based on EGFP fluorescence, we made 4,579 presexed XX*↔XY aggregation chimeric embryos, transplanted them to pseudopregnant females, and obtained 1,744 pups (Fig. 1*A*). Among the pups, 1,202 were born as males (69%) and 542 as females (31%), defined by their external genital reproductive tract anatomy. Gonadal hermaphroditism was present in 6.1% and 4.8% of grossly phenotypic males and females, respectively.

Tagging of the X chromosome by the ubiquitously expressed

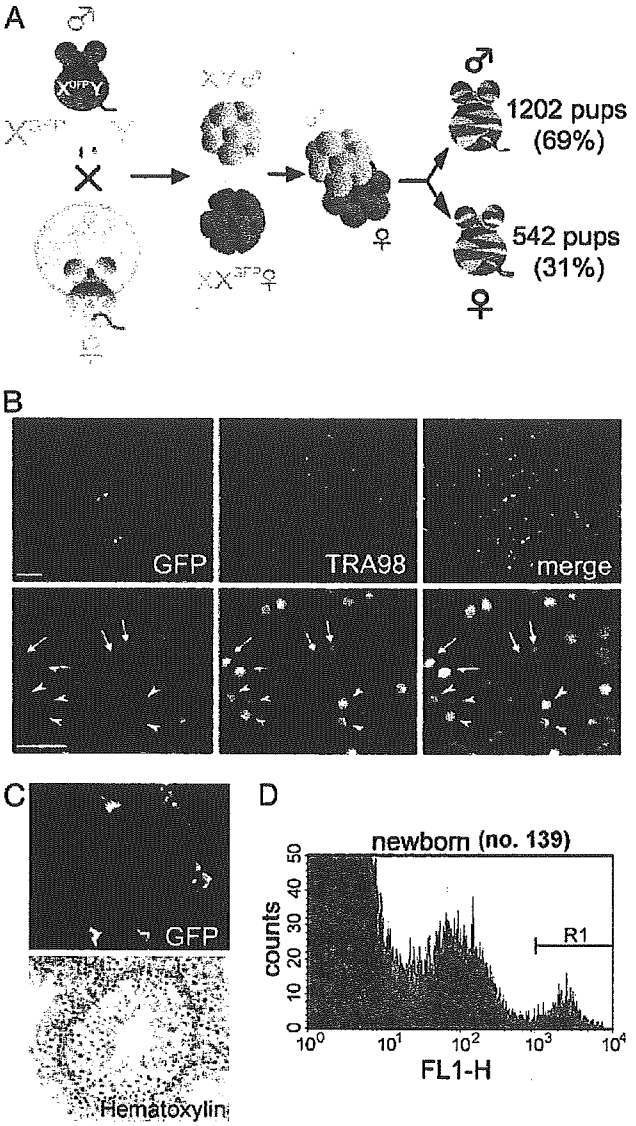

Fig. 1. XX*↔XY chimeras containing XX* cells in their testes. (*A*) Strategy of producing XX*↔XY chimera. Males containing the EGFP transgene on the X chromosome were bred with wild-type females. The male and female embryos were separated, and XX*↔XY chimera embryos were made by aggregation. These embryos were transferred to pseudopregnant females. (*B*) A testicular section from a newborn XX*↔XY chimera (no. 50). (*Upper Left*) EGFP-positive XX cells. (Scale bar: 50 μm.) (*Upper Center*) Immunolabeling (red) for TRA98, a germ cell-specific antigen. (*Lower*) Higher magnification showing XX* cells (arrows) and XY germ cells (arrowheads) in seminiferous tubules. (Scale bar: 50 μm.) (*C*) Testicular section from a 5-week-old sexually mature XX*↔XY chimera (no. 50). XX* Sertoli cells are present (*Upper*); however, XX* spermatogenic cells are absent. (*D*) Flow cytometric analysis of newborn testicular cells from the no. 139 mouse line. The forward-scatter and side-scatter dot-plot gated fraction was shown to divide into three peaks (negative, medium, and bright) in which the brightest peak consisted of >98% germ cells, proven by TRA98 staining (see *Results*).

EGFP transgene allowed us to trace XX* cells residing in testes. Numerous TRA98-positive green (XX*) cells inside the seminiferous tubules were present at birth, indicative of germ-line cells (Fig. 1*B*). However, at 5 weeks of age, no XX* spermatogenic cells were found in testes observed, despite the presence of XX* Sertoli cells (based on their characteristic shape) inside the

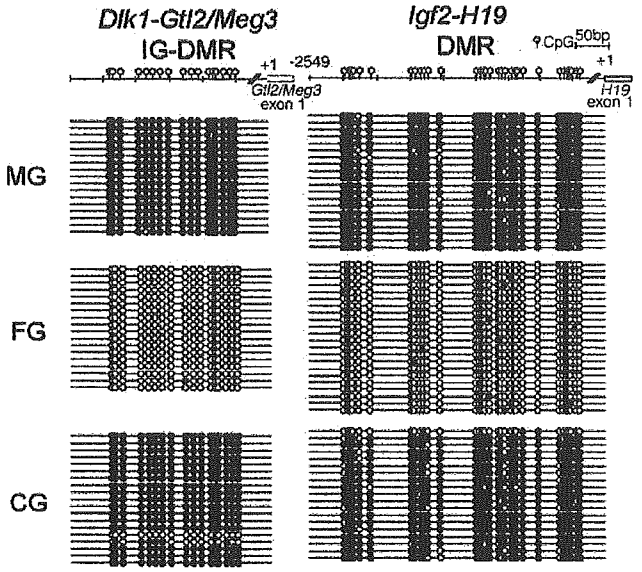

Fig. 2. Characterization of germ cells in testes of newborn XX*↔XY chimera (no. 139). DMR methylation of paternal methylated genes *Dlk1-Gtl2/Meg3* and *Igf2-H19* in newborn germ cells, analyzed by bisulfite genomic sequencing. Filled ovals indicate methylated CpGs, and open ovals indicate unmethylated CpGs. As expected, DMRs of spermatogonia (MG) showed hypermethylation, and oocytes (FG) showed hypomethylation. XX spermatogonia (CG) showed hypermethylation.

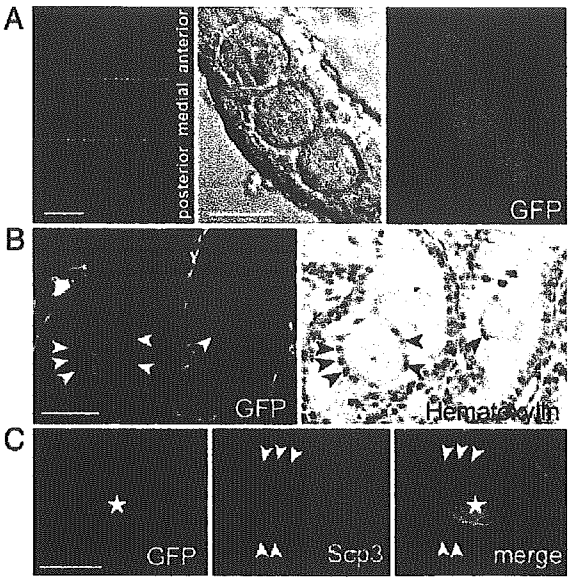

Fig. 3. Testicular eggs in seminiferous tubules. (*A*) (*Left*) Large cells in testis indicated as XX* by EGFP fluorescence (no. 139). (*Center* and *Right*) Higher magnification of three EGFP-expressing cells in a separated seminiferous tubule. (*B*) A testicular section from a 7-dpp XX*↔XY chimera. Granulosa-like cells, which surround testicular eggs, are indicated by arrowheads. (*C*) A testicular section of XX*↔XY chimera at 17 dpp (no. 139). GFP-positive testicular eggs are indicated by asterisks, and GFP-negative, SCP3-positive spermatocytes are marked by arrowheads. (Scale bars: *A Left*, 500 μm; *A Center*, *B*, and *C*, 50 μm.)

tubule and somatic cells in the interstitium in >25 independent observations (Fig. 1*C*).

Retrieval of XX* Germ Cells from XX*↔XY Chimeric Mice. To clarify the nature of XX* germ cells residing inside the seminiferous tubules in XX*↔XY chimera, we isolated germ cells tagged with X-EGFP by using a FACS. More than 30 chimeric testes were prepared, combined, and subjected to FACS analysis. The experiment was repeated on three different occasions, and the results were similar in all cases. EGFP-positive cells from XX↔XY chimeras using the no. 139 line were quantified as depicted in Fig. 1*D*. The brightest peak indicated by R1 was corrected as a germ-cell fraction after removing bright somatic cells by gating in a forward-scatter and side-scatter plot. To examine the purity of germ cells in the sorted fraction, some of these cells were attached to glass slides and immunostained with TRA98. Germ cells from newborn testes (and also germ cells collected from newborn ovaries) were successfully purified by this procedure, because 98% of thus prepared EGFP-positive cells were found to be TRA 98-positive (data not shown).

Differentiation of XX* Prospermatogonia in Chimeric Testes. To determine whether XX* germ cells recovered from testes were differentiated as prospermatogonia, the XX* germ cells were released from the seminiferous tubules and sorted by using a FACS and subjected to cell cycle analysis after staining with propidium iodide. The recovered XX* germ cells, confirmed by TRA98 staining, were 2n, as would be found in male germ cells from newborn wild-type mice (data not shown). We then analyzed the status of genomic imprinting in these cells. DMRs of *Dlk1-Gtl2/Meg3* and *Igf2-H19* were methylated in recovered XX* germ cells in a similar manner to XY germ cells in wild-type males (Fig. 2). The region analyzed for *H19* includes 500 base pairs of the imprinting control region, which is shown to be involved in the establishment of imprinting at this locus (17, 33).

Testicular Eggs Found in 1- to 4-Week-Old Chimeric Testes. We never found large cells in the XX*↔XY chimeric testis at birth. However, starting at 1 week of age, up to 100 large cells could be found inside the seminiferous tubules [19 of 46 (41%), 3 of 23 (13%), and 16 of 74 (22%) chimeric testes were found to possess large cells observed at 1, 2, and 3 weeks after birth, respectively] (Fig. 3*A*).

Although somewhat smaller than normal ovarian eggs, these cells reached 50 μm in diameter by 3 weeks, and we called them testicular eggs (Fig. 3). The testicular eggs were found mainly in the anterior (323 eggs) and posterior (142 eggs) parts of the testis, as opposed to the medial area (77 eggs) (Fig. 3*A*). (Eleven chimeric testes were examined.)

Most of the testicular eggs were surrounded by a few granulosa-like cells, but we never found the follicle-like structures seen inside the seminiferous tubules (Fig. 3*B*). There were XY (nongreen) spermatogonia near the testicular eggs, indicating the existence of normal Sertoli cells in the vicinity of the testicular eggs (Fig. 3*C*). It should also be noted that we could not find XY (nongreen) testicular eggs.

In some cases, testes were exposed by operation to allow observation under a dissecting fluorescent microscope. After confirmation of the existence of testicular eggs by surface examination of testes, we replaced the testes into the scrotum and sutured, and the mice were kept until they were 9–20 weeks of age. Sperm from five chimeric testes that possessed testicular eggs were subjected to *in vitro* fertilization and were found to have normal fertilizing ability (data not shown).

When testicular eggs were immunostained with an anti-oocyte-specific protein (ZP3) that surrounds the oocytes, they were shown to have zona pellucida structures (Fig. 4*A*). Testicular eggs were inseminated with sperm after removing the zona pellucida. Similar to ovarian eggs, the testicular eggs

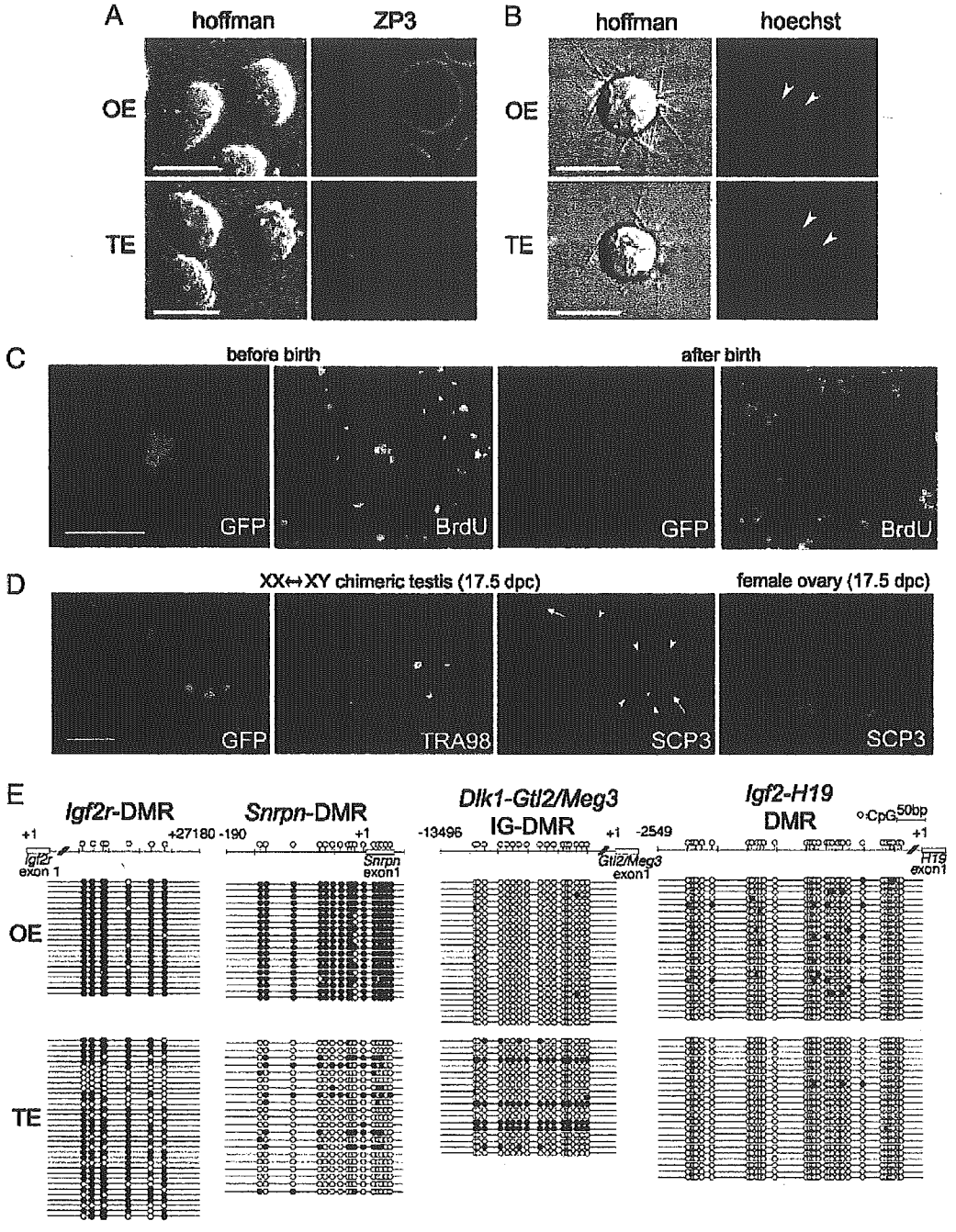

Fig. 4. Characterization of testicular eggs in chimeric testes. (*A*) Immunofluorescence staining of ZP3 in zona pellucida of testicular eggs in 1-week-old chimeric testes and oocytes in "normal" ovaries. (*B*) Sperm were added to eggs preloaded with Hoechst 33342. Fused sperm (arrowheads) are stained with Hoechst because of dye transfer from the eggs. (*C*) BrdUrd staining to detect onset of meiosis in testicular eggs. In two *Left* panels, BrdUrd was injected at 12.5 dpc, and the testicular eggs were recovered at 1 week after birth. In two *Right* panels, BrdUrd was injected every day from 0 to 5 dpp, and the testicular eggs were recovered at 6 dpp. (*D*) SCP3-positive cells in 17.5-dpc chimeric testis. EGFP indicates the XX* cells. TRA98 staining (with 7-amino-4-methylcoumarin-3-acetic acid) shows germ cells. SCP3 staining (with tetramethylrhodamine isothiocyanate) shows synaptonemal complexes. Note some XX germ cells (EGFP and TRA98 double positive) also contained SCP3 (arrowheads), whereas others did not (arrows). SCP3 staining in 17.5-dpc ovarian eggs is shown for comparison. (Scale bars: 50 μm.) (*E*) DMR methylation in maternally methylated (*Igf2r* and *Snrpn*) and paternally methylated (*Dlk1-Gtl2/Meg3* and *Igf2-H19*) genes in 3-week-old testicular eggs. Methylation of *Igf2r*-DMR, but not *Snrpn*-DMR, was similar in testicular eggs and ovarian eggs. The paternal methylated gene was almost completely nonmethylated in testicular eggs, similar to ovarian eggs.

showed the ability to fuse with sperm at as early as 1 week of age (Fig. 4*B*).

However, the fertilized eggs derived from germinal vesicle (GV)-stage testicular eggs were not able to initiate development as in the case of normal GV-stage oocytes (data not shown). To detect DNA synthesis just before meiosis, BrdUrd was repeatedly injected into newborn pups from 0 to 5 dpp. However, no BrdUrd incorporation was detected in testicular eggs, although

it was shown in other cell types (Fig. 4*C*). This lack of incorporation presumably occurs because, at birth, the testicular eggs are already 4n. BrdUrd also was injected into recipient mothers at 12.5 dpc, and the pups were analyzed at 1 week of age. Testicular eggs were brightly stained with the anti-BrdUrd antibody; male germ cells were negative because the label was diluted in prospermatogonia-differentiated cells as the result of further divisions between the time of labeling and the time of study (Fig. 4*C*). These results suggest that the testicular eggs begin meiosis at a similar time as normal eggs. Furthermore, some XX* germ cells were found to express the primary meiotic marker synaptonemal complex protein 3 (SCP3) at 17.5 dpc (Fig. 4*D*).

We manually collected >1,000 testicular eggs from chimeric testes 3 weeks after birth for an analysis of genomic imprinting. In contrast to XX spermatogonia, testicular eggs did not show paternal imprinting of *Dlk-Glt2/Meg3* and *Igf2-H19*. Instead, *Igf2r* was heavily methylated, as in normal eggs. *Snrpn* was found to remain unmethylated (Fig. 4*E*), whereas it normally becomes methylated in ovarian oocytes, suggesting that the maturation (or development) of testicular eggs is delayed. These testicular eggs remained in the testis until 4 weeks of age and then disappeared. However, the cause of this disappearance is not known.

Discussion

Sex Determination of XX Germ Cells in the Testes. A potential explanation of the formation of testicular eggs is that they are developing in regions where the masculinizing effect of XY somatic cells is being diluted by the existence of XX somatic cells. In general, germ cells are sequestered inside testis cords by 12.5 dpc, and if the sequestration is not completed, the germ cells spontaneously enter meiosis and differentiate into oocytes. Menke *et al.* (34) reported that *Stra8*, a premeiotic marker, began to be expressed from 12.5 dpc only in XX germ cells, whereas Adams and McLaren (6) reported prospermatogonia differentiated by 12.5 dpc. Thus, germ cell's sex differentiation in both male and female seems to be started on day 12.5 dpc. Once the meiotic germ cells appear in gonads, it is reported that these cells antagonize mesonephric cell migration and testis cord formation, which leads to a formation of ovotestis (35). However, the testicular eggs were always observed inside the seminiferous tubules (Fig. 3). With consideration to the above reports, we presume the testicular eggs that were always found inside the seminiferous tubules were not derived from the ovotestis area but more likely differentiated in an environment where surrounding somatic tissues are destined to differentiate into testes. It is reported that *Sry* expression and testicular cord formation emanates from the central region of the gonad (36, 37), whereas the formation of the oogenesis wave starts from the anterior part of the gonads and extends into the posterior region (34). If the differentiation of gonads begins simultaneously as male and female, the anterior part of the gonad is most likely the area where the germ cells differentiate into female. Supporting this assumption, most of the testicular eggs were found in the seminiferous tubules in the anterior and posterior poles of the testis and occasionally around the testicular surface (Fig. 3*A*). Moreover, the testis cords in which testicular eggs were located prenatally could have been incomplete or in some way abnormal because of the presence of XX somatic cells, with the cords appearing as normal testicular cords at a later stage of development. This environmental condition might have some similarity with the mesonephric rete in the testis of fetal sex-reversed mice. McLaren (38) reported that the existence of the second X chromosome (XX) renders germ cells more susceptible to the meiosis-inducing influence from such an environment. We therefore presume that a cascade of molecular and cellular events leading to oogenesis began in XX germ cells in testes before environmental factors from the testicular cords prohibited meiosis and resulted in testicular eggs.

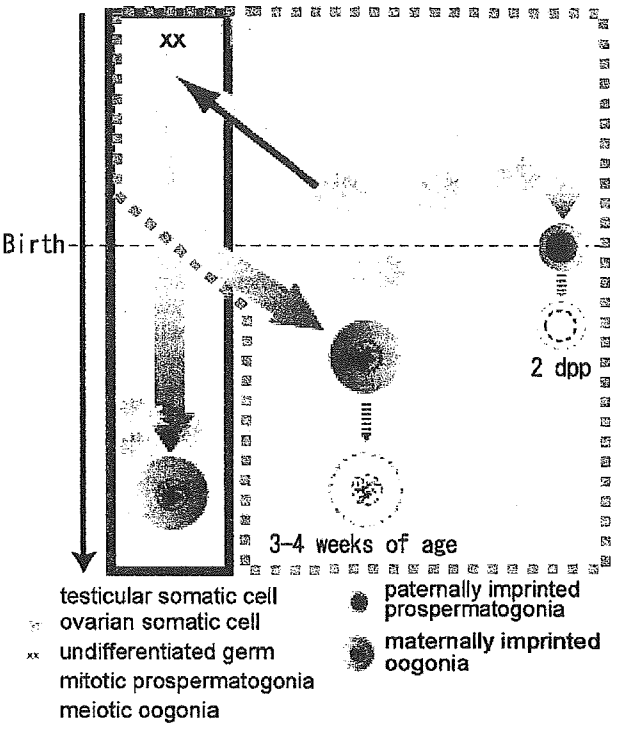

Fig. 5. XX germ cells are reported to develop as spermatogonia when deposited in a testicular environment (6, 10). However, proof of male type differentiation in molecular bases was not available. As shown in the present study, once XX germ cells were inhibited from entering meiosis, they were demonstrated to acquire paternal imprinting, which indicates the development of XX prospermatogonia. In 1-dpp testes, we found approximately as many spermatogonia surviving as in the 0-dpp testes. However, the XX* spermatogonia were seldom seen at 2 dpp (data not shown). The reason for this disappearance is not known. Occasionally, some XX germ cells initiated meiosis in seminiferous tubules in their embryonic stage and were arrested in 4n stage. Despite continuous exposure to male factors inside seminiferous tubules during the embryonic stage, these cells did not acquire paternal imprinting as XX prospermatogonia. Instead, they resumed meiosis after birth and obtained a maternal imprinting pattern in the testicular environment. Because the maternal imprinting starts after birth in the growing oocytes, the imprinting in testicular eggs may also start after birth, together with their growth in size. Taking these facts together, we postulate that the pattern of genomic imprinting is designated when the germ cells choose the sex to develop at ≈12.5 dpc and that it is not influenced by environmental factors when methylation takes place.

Genomic Imprinting of XX* Germ Cells in Testis. Many XX* germ cells that were supposed to be prospermatogonia were found in XX*↔XY chimeric testes. However, there was little information about these cells being prospermatogonia. Recently, Durcova-Hills *et al.* (39) reported using sex-reversal mice in which the imprinted genes *Igf2* and *H19* were methylated more heavily in embryonic germ-cell lines established with an XY sex chromosome constitution than in those with an XX sex chromosome constitution, irrespective of the phenotypic sex of the genital ridge from which the embryonic germ cells (EGCs) had been derived. They concluded that the aberrant sex-specific methylation of these genes in EGCs is intrinsic and cell-autonomous and is not due to any influence of the genital ridge somatic cells (39). In contrast, the XX* spermatogonia from XX*↔XY chimeric testes clearly showed a male-type methylation pattern

in imprinted genes, which was possibly influenced by somatic cells, despite their female set of chromosomes (Fig. 2). One of the reasons for this discrepancy may be the types of cells examined (XX* spermatogonia vs. EGCs). Moreover, Durcova-Hills *et al.* (39) examined the genomic imprinting of EGCs at 11.5 dpc, which is about the time of the elimination of genomic imprinting. In contrast, we examined the status of genomic imprinting in XX* germ cells at 0 dpp.

Based on the observation of cell size, a small number of XX germ cells were reported to have developed as testicular eggs in XXsxr sex-reversal mice testes (40). In the present experiment, taking advantage of EGFP tagging, these matured (or grown-up) XX* cells in the testes were recovered and were demonstrated to have zona pellucida and fusing ability with sperm. These characteristics apparently appeared during the growth of "eggs" inside seminiferous tubules after birth. This finding indicates that the testicular environment did not inhibit resuming of oogenesis and subsequent oocyte maturation in seminiferous tubules. Moreover, it should be noted that the testicular eggs must have sequestered inside seminiferous tubules and been exposed to male factors from the beginning of meiosis in the embryonic stage (Fig. 4 *C* and *D*) to the methylation-acquiring period after birth (Fig. 4*E*). The data described in the present study indicate that the sex-specific methylation pattern does not always follow the chromosomal constitution or the environmental conditions where the germ cells reside. Instead, the imprinting pattern seems to be defined by the sex that was chosen by the germ cells at their early stage of development (Fig. 5).

These findings may relate to the symptoms of XX human males [estimated to occur in 1/20,000–1/25,000 births (41)] and Klinefelter syndrome patients [XXY males are estimated to occur in 1/500–1/1,000 births (42)], in which germ cells that contain two X chromosomes are reported to disappear during maturation (7, 13). Because the experimental model that we established allowed us to recover live germ cells, it can be used to investigate more detailed mechanisms of male infertility and sex differentiation in germ cells in general.

We thank Dr. Yoshitake Nishimune (Osaka University, Osaka) for his generous gift of the TRA98 antibody used in this study. In addition, we thank Dr. Susan S. Suarez and Dr. Stuart B. Moss for critically reading the manuscript. This work was supported by grants from the Ministry of Education, Culture, Sports, Science, and Technology of Japan (MEXT) (15080207) and the 21st Century Center of Excellence Program of MEXT. J.L. is a Fellow of the Japan Society for the Promotion of Science.

1. Merchant-Larios, H. & Moreno-Mendoza, N. (2001) *Arch. Med. Res.* **32,** 553–558.
2. Albrecht, K. H., Young, M., Washburn, L. L. & Eicher, E. M. (2003) *Genetics* **164,** 277–288.
3. Lee, C. H. & Taketo, T. (2001) *Genesis* **30,** 7–11.
4. Lovell-Badge, R. & Robertson, E. (1990) *Development (Cambridge, U.K.)* **109,** 635–646.
5. Koopman, P., Gubbay, J., Vivian, N., Goodfellow, P. & Lovell-Badge, R. (1991) *Nature* **351,** 117–121.
6. Adams, I. R. & McLaren, A. (2002) *Development (Cambridge, U.K.)* **129,** 1155–1164.
7. McLaren, A. (1995) *Philos. Trans. R. Soc. London B Biol. Sci.* **350,** 229–233.
8. McLaren, A. & Southee, D. (1997) *Dev. Biol.* **187,** 107–113.
9. Bronson, S. K., Smithies, O. & Mascarello, J. T. (1995) *Proc. Natl. Acad. Sci. USA* **92,** 3120–3123.
10. Palmer, S. J. & Burgoyne, P. S. (1991) *Development (Cambridge, U.K.)* **112,** 265–268.
11. Burgoyne, P. S., Levy, E. R. & McLaren, A. (1986) *Nature* **320,** 170–172.
12. Levy, E. R. & Burgoyne, P. S. (1986) *Cytogenet. Cell Genet.* **42,** 208–213.
13. Lue, Y., Rao, P. N., Sinha Hikim, A. P., Im, M., Salameh, W. A., Yen, P. H., Wang, C. & Swerdloff, R. S. (2001) *Endocrinology* **142,** 1461–1470.
14. Mroz, K., Carrel, L. & Hunt, P. A. (1999) *Dev. Biol.* **207,** 229–238.
15. Surani, M. A. (2001) *Nature* **414,** 122–128.
16. Davis, T. L., Trasler, J. M., Moss, S. B., Yang, G. J. & Bartolomei, M. S. (1999) *Genomics* **58,** 18–28.
17. Ueda, T., Abe, K., Miura, A., Yuzuriha, M., Zubair, M., Noguchi, M., Niwa, K., Kawase, Y., Kono, T., Matsuda, Y., *et al.* (2000) *Genes Cells* **5,** 649–659.
18. Obata, Y. & Kono, T. (2002) *J. Biol. Chem.* **277,** 5285–5289.
19. Lucifero, D., Mertineit, C., Clarke, H. J., Bestor, T. H. & Trasler, J. M. (2002) *Genomics* **79,** 530–538.
20. Nakanishi, T., Kuroiwa, A., Yamada, S., Isotani, A., Yamashita, A., Tairaka, A., Hayashi, T., Takagi, T., Ikawa, M., Matsuda, Y. & Okabe, M. (2002) *Genomics* **80,** 564–574.
21. Okabe, M., Ikawa, M., Kominami, K., Nakanishi, T. & Nishimune, Y. (1997) *FEBS Lett.* **407,** 313–319.
22. Hadjantonakis, A. K., Gertsenstein, M., Ikawa, M., Okabe, M. & Nagy, A. (1998) *Nat. Genet.* **19,** 220–222.
23. McMahon, A., Fosten, M. & Monk, M. (1981) *J. Embryol. Exp. Morphol.* **64,** 251–258.
24. Monk, M. & McLaren, A. (1981) *J. Embryol. Exp. Morphol.* **63,** 75–84.
25. McLaren, A. & Monk, M. (1981) *J. Reprod. Fertil.* **63,** 533–537.
26. Jamieson, R. V., Zhou, S. X., Wheatley, S. C., Koopman, P. & Tam, P. P. (1998) *Dev. Biol.* **199,** 235–244.
27. Tam, P. P., Zhou, S. X. & Tan, S. S. (1994) *Development (Cambridge, U.K.)* **120,** 2925–2932.
28. Clerc, P. & Avner, P. (2000) *Science* **290,** 1518–1519.
29. Zhou, L., Yoshimura, Y., Huang, Y., Suzuki, R., Yokoyama, M., Okabe, M. & Shimamura, M. (2000) *Immunology* **101,** 570–580.
30. Nagy, A., Rossant, J., Nagy, R., Abramow-Newerly, W. & Roder, J. C. (1993) *Proc. Natl. Acad. Sci. USA* **90,** 8424–8428.
31. Ho, Y., Wigglesworth, K., Eppig, J. J. & Schultz, R. M. (1995) *Mol. Reprod. Dev.* **41,** 232–238.
32. Ohta, H., Yomogida, K., Dohmae, K. & Nishimune, Y. (2000) *Development (Cambridge, U.K.)* **127,** 2125–2131.
33. Lee, J., Inoue, K., Ono, R., Ogonuki, N., Kohda, T., Kaneko-Ishino, T., Ogura, A. & Ishino, F. (2002) *Development (Cambridge, U.K.)* **129,** 1807–1817.
34. Menke, D. B., Koubova, J. & Page, D. C. (2003) *Dev. Biol.* **262,** 303–312.
35. Yao, H. H., DiNapoli, L. & Capel, B. (2003) *Development (Cambridge, U.K.)* **130,** 5895–5902.
36. Albrecht, K. H. & Eicher, E. M. (2001) *Dev. Biol.* **240,** 92–107.
37. Bullejos, M. & Koopman, P. (2001) *Dev. Dyn.* **221,** 201–205.
38. McLaren, A. (1981) *J. Reprod. Fertil.* **61,** 461–467.
39. Durcova-Hills, G., Burgoyne, P. & McLaren, A. (2004) *Dev. Biol.* **268,** 105–110.
40. McLaren, A. (1980) *Nature* **283,** 688–689.
41. de la Chapelle, A. (1981) *Hum. Genet.* **58,** 105–116.
42. Philip, J., Lundsteen, C., Owen, D. & Hirschhorn, K. (1976) *Am. J. Hum. Genet.* **28,** 404–411.

Available online at www.sciencedirect.com
SCIENCE DIRECT®
Journal of BIOTECHNOLOGY
ELSEVIER
Journal of Biotechnology 118 (2005) 123–134
www.elsevier.com/locate/jbiotec

Multi-gene Gateway clone design for expression of multiple heterologous genes in living cells: Conditional gene expression at near physiological levels

Kazuhide Yahata[a,c], Hiroe Kishine[a], Takefumi Sone[a], Yukari Sasaki[a,d], Junko Hotta[a], Jonathan D. Chesnut[b], Masaru Okabe[c], Fumio Imamoto[a,*]

[a] *Department of Molecular Biology, Research Institute for Microbial Diseases, Osaka University, 3-1 Yamadaoka, Suita, Osaka 565-0871, Japan*
[b] *Invitrogen Corporation, Carlsbad, CA, USA*
[c] *Department of Experimental Genome Research, Faculty of Pharmaceutical Sciences, Osaka University, 3-1 Yamadaoka, Suita, Osaka 565-0871, Japan*
[d] *Department of Bacterial Infections, Faculty of Pharmaceutical Sciences, Osaka University, 3-1 Yamadaoka, Suita, Osaka 565-0871, Japan*

Received 27 October 2004; received in revised form 9 December 2004; accepted 21 February 2005

Abstract

Using Multisite Gateway five-DNA-fragment constructs vectors that enable expression of two tandemly situated cDNAs on a single plasmid were developed. Heterologous protein production in cells was achieved by modulating respective cDNA expression to pre-determined and different levels. Optimization of cDNA expression at near physiological protein levels was achieved using promoters from four cell cycle-dependent genes. In comparison with conventionally available promoters, *EF-1α* or CMV, the promoters used in this study were able to modulate cDNA expression levels over a magnitude of approximately 10 or 100-fold, respectively. In transiently transfected cells, two different proteins (CPα1 and CPβ2), which form a heterodimer, each labeled with a different-colored fluorescent protein, were successfully synthesized at pre-determined levels from their respective cDNAs. The above vectors were designed to contain an FRT/Flp recombination site for integration onto chromosomes and for establishment of stable clones in HeLa cells by site-specific recombination. In the stable transformant cells produced only about 4% of the protein production levels measured in the transiently transformed cells. The biological significance of these observations is discussed.

Keywords: Multisite Gateway cloning; Multi-gene expression clone; Simultaneous introduction of multiple cDNAs; Low expression promoters; Controllable expression of transgenes

* Corresponding author. Tel.: +81 6 6879 8325; fax: +81 6 6879 8325.
E-mail address: qzi04457@nifty.com (F. Imamoto).

0168-1656/$ – see front matter © 2005 Elsevier B.V. All rights reserved.
doi:10.1016/j.jbiotec.2005.02.020

1. Introduction

A matter of growing interest and emphasis in recent genome science and cell biology has been the development of technologies to introduce target genes into a specific site on the chromosome without impairing intracellular proteomic function and cellular physiology. The conventional method of transient transfection cannot control for the number of plasmids introduced to cells. This could potentially lead to protein overproduction and artificial and non-physiological effects. Furthermore, often the transformant phenotype tends to be lost during cell divisions. Some target genes carried by the plasmids may be inserted into random sites on the chromosome. Their expression generally cannot be predicted or reproduced and many of them not expressed due to their position in heterochromatic regions or due to negative interactions between the transgene and adjacent regulatory elements (Feng et al., 1999; Villemure et al., 2001). In most experiments with stable transformants, appropriately expressing cells are isolated from the population, though there often are large differences in protein expression between clones due to lack of control of chromosomal location.

In order to perform systematic stable transformation, use of a site-directed recombination systems such as Flp/FRT and Cre/lox is desirable, (Xu and Rubin, 1993). Further development of such systems would be advisable for application to a wider array of mammalian cell lines and embryonic stem cells.

It would also be desirable to establish optimal conditions for the introduction of multiple genes stoichiometrically and simultaneously into an active chromatin site on the chromosome. The conventional method of co-transfection with two or more single-gene carrying plasmids as a mixture has significant shortcomings. Often the resultant transformant cell population after co-transfection of, for example, two different types of recombinant plasmids is frequently a mixture of doubly transfected and singly transfected cells. Further, the doubly transfected cells may not harbor equal numbers of two respective plasmids.

We reported previously that Multisite Gateway technology makes it possible to construct tandem structures containing two to four different cDNA clones in a single plasmid. These constructs have been successfully used for simultaneously introducing multiple heterologous genes into living cells (Sone et al., 2005). Optimization of their expression levels would be necessary for proteomic research where measurement of intracellular trafficking and interaction of functional proteins in a nearly physiological context is desired.

In this paper, we present experimental results describing simultaneous introduction of two heterologous cDNAs labeled differentially by the fluorescent protein tags and controllable expression of these respective genes in both transient and stable transformant cells.

2. Materials and methods

2.1. Entry clones

The Entry clones (pENTR) containing promoter DNA and fluorescent protein ORFs were constructed as follows. Four different types of low-expression promoters for *cyclin E*, *cdc2*, *cyclin B1* and *aurora A* genes were prepared by PCR amplification with *att*B-flanked or *att*B-*Hind*III-flanked oligonucleotide primers (Table 1) using human genomic DNA extracted from Jurkat cells as template (Sambrook et al., 2001). For construction of the Entry clones containing the *EF-1α* and *CMV* promoters, the destination vectors of pEF5/FRT/V5-DEST (Invitrogen Corp.) and pDEST12.2 (Invitrogen Corp.) were used, respectively, as DNA templates for *att*B-flanked adapter PCR-amplification (Sone et al., 2005). For fluorescent proteins, EGFP (Cormack et al., 1996; Zhang et al., 1996) (BD Biosciences Clontech Inc.; GenBank accession no.: U55763) and mRFP1 (Campbell et al., 2002) (GenBank accession no.: AF506027) were employed in this report. The recombinant plasmids containing the respective fluorescent protein ORFs, pEGFP-C1 (BD Biosciences Clontech Inc.) and pRSET$_B$-mRFP1, were used as templates for PCR. The *att*B-flanked PCR products were recombined with the Donor vectors containing the corresponding *att*P signals in BP reactions to generate the Entry clones containing the promoters and fluorescent protein tags. The Entry clones constructed with the promoters and EGFP are listed in Table 2.

The Entry clones used for construction of two types of the fused cDNA tandem Expression clones (see Fig. 1) were pENTR-L1- *cpβ2*-B3- *EGFP*-*B6-*pA*-P$_{EF1α}$-B5-*mRFP1*-B4-*cpα1*-*L2 and pENTR-L1- *cpβ2*-B3- *EGFP*- *B6-*pA*-P$_{cdc2}$-B5-*mRFP1*-B4-*cpα1*-*L2. The former Entry clone was prepared

Table 1
Primers used to create PCR-products flanked by two different *att*B sites

B1-$P_{auroraA}$-Fw	GGGG**CAAGTTTGTACAAAAAAGCAG**TCACATGAGAGATTAGAGGC
B6-$P_{auroraA}$-Rv	GGGG**CAACTTTGTATTAAAAAGTTG**CTCTAGCTGTAATAAGTAAC
B1-P_{cdc2}-Fw	GGGG**CAAGTTTGTACAAAAAAGCAG**CAGCTGCGCTGGAGGCTGAG
B6-P_{cdc2}-Rv	GGGG**CAACTTTGTATTAAAAAGTTG**CGGCTTATTATTCCGCGGCG
B3-*Hind*III-P_{cdc2}-Fw	GG**CAACTTTGTATAATAAAGTTG**AAGCTTCAGCTGCGCTGGAGGCTGA
B4R-*Hind*III-P_{cdc2}-Rv	GG**CAACTTTTCTATACAAAGTTG**AAGCTTCGGCTTATTATTCCGCGGC
B1-$P_{cyclinB1}$-Fw	GGGG**CAAGTTTGTACAAAAAAGCAG**CGCCTTCGCGCGATCGCCCTG
B6-$P_{cyclinB1}$-Rv	GGGG**CAACTTTGTATTAAAAAGTTG**GGCTTCCTCTTCACCAGGCAG
B1-$P_{cyclinE}$-Fw	GGGG**CAAGTTTGTACAAAAAAGCAG**GCCTGGCGGGACAGCGCGCG
B6-$P_{cyclinE}$-Rv	GGGG**CAACTTTGTATTAAAAAGTTG**GATGGGGCTGCTCCGGCCTG
B3-*Hind*III-$P_{cyclinE}$-Fw	GG**CAACTTTGTATAATAAAGTTG**AAGCTTGCCTGGCGGGACAGCGCGC
B4R-*Hind*III-$P_{cyclinE}$-Rv	GG**CAACTTTTCTATACAAAGTTG**AAGCTTGATGGGGCTGCTCCGGCCT
B1-P_{CMV}-Fw	GGGG**CAAGTTTGTACAAAAAAGCAG**CGTTACATAACTTACGGTAAA
B6-P_{CMV}-Rv	GGGG**CAACTTTGTATTAAAAAGTTG**CGGAGGCTGGATCGGTCCCGG
B1-$P_{EF1\alpha}$-Fw	GGGG**CAAGTTTGTACAAAAAAGCAG**CGTGAGGCTCCGGTGCCCGTC
B6-$P_{EF1\alpha}$-Rv	GGGG**CAACTTTGTATTAAAAAGTTG**TCACGACACCTGAAATGGAAG
B6r-*EGFP*-Fw	GGGG**CAACTTTTTAATACAAAGTTG**ATG TGAGCAAGGGCGAGGAG
B2*-*EGFP*-Rv	GGGGA**CCACTTTGTACAAGAAAGCTG**TTA TTGTACAGCTCGTCCATGCC

The *att*B sites are shown in bold and are underlined. The Shine-Dalgarno and Kozak consensus sequences (SDK) are shown in plain font and underlined. Initiation codons, ATG and stop codons, TAA are shown with open boxes. The name of the primers are indicated as "attached signal sequence (Bx or SDK)-gene specific sequence (*aurora A*, *cdc2*, *cyclin E*, etc.)-orientation, forward (Fw) or reverse (Rv)". The primers that contain a stop codon are labeled with an asterisk (*) in their names. The other interpretations are as in the experimental procedures.

from an Expression clone, pEF5/FRT/V5-B1- *cpβ2*-B3- *EGFP*- *B6-*pA*-$P_{EF1\alpha}$-B5-*mRFP1*-B4-*cpα1*-*B2 (described in Fig. 3 of Sone et al., 2005), by BP reaction with pDONR201 (Invitrogen Corp.). The latter Entry clone was constructed by replacing the $P_{EF1\alpha}$-DNA in pENTR-L1- *cpβ2*- B3- *EGFP*- *B6-*pA*-$P_{EF1\alpha}$-B5-*mRFP1*-B4-*cpα1*-*L2 with the P_{cdc2}-DNA. This replacement was carried out by first inserting the *att*B-*Hind*III-flanked adapter PCR fragment amplified from pENTR-L1-P_{cdc2}-L6 into a *Hinc* II site of pUC18, thus producing pUC-B3-*Hind*III-P_{cdc2}-*Hind*III-B4r. Then the pUC-B3-*Hind*III-P_{cdc2}-*Hind*III-B4r was used for replacing the $P_{EF1\alpha}$-DNA flanked by *Hind*III sites on the pENTR-L1- *cpβ2*- B3- *EGFP* *B6-*pA*-$P_{EF1\alpha}$-B5-*mRFP1*-B4-*cpα1*-* with the *Hind*III-P_{cdc2}-*Hind*III fragment by ligation.

Table 2
List of the vectors and clones used

Entry clones	Expression clones	
pENTR-L1-$P_{auroraA}$-L6	pFRT/V5-B1-$P_{auroraA}$-B6-SDK-*EGFP*-*L2	(pEXPR-$P_{auroraA}$-*EGFP*)
pENTR-L1-P_{cdc2}-L6	pFRT/V5-B1-P_{cdc2}-B6-SDK-*EGFP*-*L2	(pEXPR-P_{cdc2}-*EGFP*)
pENTR-L1-$P_{cyclinB1}$-L6	pFRT/V5-B1-$P_{cyclinB1}$-B6-SDK-*EGFP*-*L2	(pEXPR-$P_{cyclinB1}$- *EGFP*)
pENTR-L1-$P_{cyclinE}$-*L6*	pFRT/V5-B1-$P_{cyclinE}$-B6-SDK-*EGFP*-*L2	(pEXPR-$P_{cyclinE}$-*EGFP*)
pENTR-L1-P_{CMV}-L6	pFRT/V5-B1-$P_{EF1\alpha}$-B6-SDK-*EGFP*-*L2	(pEXPR-$P_{EF1\alpha}$-*EGFP*)
pENTR-L1-$P_{EF1\alpha}$-L6	pFRT/V5-B1-P_{CMV}-B6-SDK-*EGFP*-*L2	(pEXPR-P_{CMV}-*EGFP*)
pENTR-R6-SDK-*EGFP*-*L2	pEF5/FRT/V5-B1-*cpβ2*-B3-*EGFP*-*B2	(pEXPR-*cpβ2-EGFP*)
pENTR-L1-*EGFP*-B3-*cpβ2*-*B6-*pA*-$P_{EF1\alpha}$-B5-*mRFP1*-B4-cpαl-*L2	pEF5/FRT/V5-B1-*mRFP1*-B3-*cpα1*-*B2	(pEXPR-*mRFPl-cpα1*)
	p*cyclin E*/FRT/V5-B1-*cpβ2*-B3-*EGFP*-*B6-*pA*-$P_{EF1\alpha}$-B5-*mRFP1*-B4-*cpα1*-*B2	(pEXPR-*cyclin E/EF1*)
pENTR-L1-*EGFP*-B3-*cpβ2*-*B6-*pA*-P_{cdc2}-B5-*mRFP1*-B4-cpαl-*L2	p*cyclin E*/FRT/V5-B1-*cpβ2*-B3-*EGFP*-*B6-*pA*-P_{cdc2}-B5-*mRFP1*-B4-*cpα1*-*B2	(*pEXPR-cyclin E/cdc2*)

The idiomatic names of the Expression clones used in the present experiments are shown in parentheses. The stop codons are labeled with an asterisk (*) in their names. The other interpretations are as in the experimental procedures.

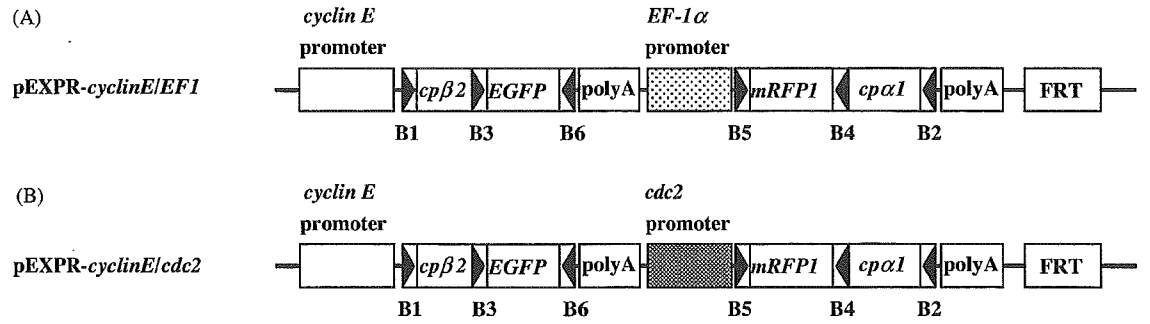

Fig. 1. Two types of fused cDNA tandem Expression clones. (A) Two cDNAs, *cpβ2* and *cpα1*, were fused to the EGFP-ORF at the C-terminus of the *cpβ2*-cDNA and mRFP1-ORF at the N-terminus of the *cpα1*-cDNA, respectively. The former fusion DNA was joined with the *cyclin E* promoter and the latter fusion DNA were joined with the *EF-1α* promoter. (B) A similar construct to (A), except that the *EF-1α* promoter was replaced with *cdc2* promoter.

The Entry vector containing the actin capping protein subunits, CPα1 and CPβ2 (Barron-Casella et al., 1995) (GenBank accession nos.: U56637 and U03271) were constructed according to the procedures reported by Sone et al. (2005). The oligo-DNA primers used for PCR amplification are listed in Table 1.

2.2. Destination vectors

Construction of the Destination vector, p*cyclin E*/FRT/V5-DEST was carried out by replacing the *EF-1α* promoter from pEF5/FRT/V5-DEST with the *cyclin E* promoter. By inserting the *att*B-*Hind*III-flanked adapter PCR fragment amplified from pENTR-L1-$P_{cyclinE}$-L6 into a *Hinc*II site of pUC18, the pUC-B3-*Hind*III-$P_{cyclinE}$-*Hind*III-B4r was produced. Then this vector was used for replacing the $P_{EF1\alpha}$-DNA flankd by *Hind* III sites on the pEF5/FRT/V5-DEST with the *Hind*III-$P_{cyclinE}$-*Hind*III fragment by ligation. The oligo-DNA primer used for PCR amplification is listed in Table 1.

2.3. Expression clones

For construction of Expression clones (Fig. 1), each of which carries two fused cDNAs as tandem cassettes, *cpβ2-EGFP* and *mRFP1-cpα1*, transcribed by *cyclin E* and *EF-1α* promoters, respectively, or the same cassette driven by *cyclin E* and *cdc2* promoter, respectively, a Destination vector, p*cyclin E*/FRT/V5-DEST, was used with pENTR-L1- *cpβ2*- B3- *EGFP*- *B6-*pA*-$P_{EF1\alpha}$-B5-*mRFP1*-B4-*cpα1*-*L2 or pENTR-L1- *cpβ2*- B3-*EGFP*- *B6-*pA*-P_{cdc2}-B5-*mRFP1*-B4-*cpα1*-*L2 in an LR reaction. The other Expression clones used in this report were constructed with the respective Entry clones and Destination vector, described in the foregoing (Section 2.2). The Expression clones (pEXPR) constructed were listed in Table 2.

2.4. Bacterial hosts and transformation

For the construction of Donor and Dest vectors containing the *ccd*B gene (Bernard et al., 1993), Library Efficiency DB3.1^{TM} Competent Cells (Invitrogen Corp.) were used. For construction of other vectors and clones without the *ccd*B gene, Max Efficiency DH10B^{TM} (Invitrogen Corp.) was used. The transformation method followed the supplier's instructions and the previous report (Sone et al., 2005). The plasmid DNA of each clone was isolated using Quantum Prep Mini Kit (Bio-Rad Laboratories) and the size and restriction enzyme digestion pattern were confirmed by agarose gel electrophoresis. The clones with the correct size and pattern were stored and used for further experiments.

2.5. Cell culture and transfection

Tissue culture cells were incubated in DMEM (Dulbecco's modified Eagle's minimum essential medium DMEM; Invitrogen Corp.) supplemented with 10% fetal bovine serum (FBS; Invitrogen Corp.) at 37 °C in 5% CO_2. Transient and stable transfection of HeLa cells was carried out using LipofectAmine Plus regents

according to the manufacture's instructions (Invitrogen Corp.).

2.6. Stable transformant cells

The stably transformed HeLa cells harboring fused cDNA Expression constructs shown in Fig. 1 were constructed according to the protocol described in the Flp-In™ System (Invitrogen Corp.) except that the lacZ-zeocin resistance gene was replaced with the blasticidin-resistance gene. HeLa cells carrying Expression clones integrated onto at least three FRT sites on the chromosome (FRT-HeLa) were selected by their hygromycin resistance. (Flp-In 293 cells purchased from Invitrogen which were zeocin resistant were also used.)

The plasmid, pFRT/Blasticidin, was constructed from pFRT/lacZeo (Invitrogen Corp.) by replacing the *Xba*I-*Sma*I fragment with the *Xba*I-FRT-Blasticidin^R-*Sma*I PCR fragment synthesized by PCR amplification from pcDNA6/TR (Invitrogen Corp.) with a set of synthetic forward and reverse oligonucleotide primers, XbaI-FRT-Bla-Fw (5′-tctagaaagtataggaacttcagccaagcctttgtctcaagaag-3′) and SmaI-Bla-Rv (5′-cccgggcggccacgaagtgcttagcc-3′), respectively. For constructing the blasticidin-resistant HeLa cell line, transfection of the pFRT/Blasticidin (linearized at the *Apa* I site) into the cells was performed. After 48 h of transfection, the medium was replaced with the fresh medium containing 2 μg/ml Blasticidin S HCl (Invitrogen Corp.). After 1–2 weeks, at least 20 blasticidin-resistant foci were subcloned and several clones were expanded finally. One of the blasticidin-resistant clones (HeLa-FRT) was used for establishment of stable transformant cells carrying the transgenes encoding CPβ2-EGFP and mRFP1-CPα1. The number of genomically integrated FRT sites in each blasticidin-resistant cell clone was determined by Southern blot analysis (Sambrook et al., 2001). The expression vectors, pEXPR-*cyclin E/EF1* or pEXPR-*cyclin E/cdc2* and the Flp recombinase expression plasmid, pOG44 (Invitrogen Corp.) were co-transfected into the FRT-HeLa cells or Flp-In 293 cells (Invitrogen Corp.), according to the manufacture's instructions (Invitrogen Corp.). After 48 h, the medium was exchanged with fresh medium containing 200 μg/ml Hygromycin B (Invitrogen Corp.). After 1–2 weeks, 4–6 hygromycin-resistant foci were subcloned and the hygromycin-resistant and blasticidin-sensitive clones or hygromycin-resistant and zeocin-sensitive clones (for Flp-In 293 cells) were selected.

2.7. Living cell imaging

Cells were grown on glass bottom dishes (Iwaki schitec) for 24 h prior to use. Prior to imaging, the medium was removed and replaced with Opti-MEM I (Invitrogen Corp.) without phenol red. Cells were observed with a fluorescence microscope (DIAPHOTO300; Nikon) with a filter wheel (Ludl Electronic Products) equipped with filter sets for CFP/YFP/Cy5 (86008v1; Chroma Technology Corp.) and BFP/GFP/DsRed (86009; Chroma Technology Corp.) and a cooled CCD camera (ORCA-ER; Hamamatsu Photonics) (Figs. 2 and 3). To measure the fluorescence images, three images from each transfected cell population were analyzed by ImageJ imaging analysis software (Freely available; http://rsb.info.nih.gov/ij/) and the measured average intensity produced by fluorescent cells was estimated by setting a threshold. Confocal microscope Imaging was performed using Zeiss LSM510 confocal microscope (Figs. 2 and 4).

2.8. Immunoprecipitation

Cells were lysed with TBST buffer containing 20 mM Tris–HCl (pH 8.0), 150 mM NaCl and 0.1% Tween 20. Normal rabbit serum was then added to the cell lysate and incubated for 1 h. The cell lysate was centrifuged and the supernatant was incubated with protein G-Sepharose beads (Amersham Biosciences) for 1 h. Anti-mRFP1 antibody (provided by Dr. Hiromitsu Tanaka, Research Institute for Microbial Diseases, Osaka University) was then added to the supernatant and incubated overnight. After centrifugation, immune complexes were adsorbed to protein G-Shpharose beads by incubation for 2 h. After five washes with RIPA buffer containing 150 mM NaCl, 1% NP-40, 0.5% deoxycholate, 0.1% SDS and 50 mM Tris–HCl (pH 8.0), the immunoprecipitates were analyzed by immunoblot analysis using an anti-GFP antibody (Molecular Probes). Immunoblot analysis was essentially performed as described previously (Kishine et al., 2002).

2.9. Antibody production

The mRFP1 cDNA fragment containing its entire coding region was PCR amplified with a set of synthetic oligonucleotide primers, mrfp-1 (5′-catgccatggcctcctccgaggacgt-3′) containing an *Nco* I linker and mrfp2 (5′-gggatatctcctccgaggacgtcatc-3′) containing an *EcoR* V linker, using the plasmid, pRSET$_B$-mRFP1 (provided by Dr. Roger Y. Tsien, UCSD, USA), as the template. The PCR product was digested with *Nco* I and *EcoR* V, and subcloned into pET30a (Novagen, WI, USA). The protein tagged with hexahistidines at the N-terminus was expressed in *E. coli* BL21 by induction with IPTG, purified on Ni-NTA mini columns (QIAGEN) as instructed by the manufacturer's protocol, and used to raise polyclonal antisera in rabbits along with Freund's Adjuvant (Difco Laboratories Inc.). Complete and incomplete Freund's Adjuvant was used for the first, and subsequent immunizations, respectively. Recombinant mRFP1 was used to immunize two Japanese white rabbits. Polyclonal antisera were obtained by injection of each of the antigens, followed by three booster injections at 3-week intervals, for a total of four injections. Each anti-serum specifically reacted with its antigen by immunoblot analysis.

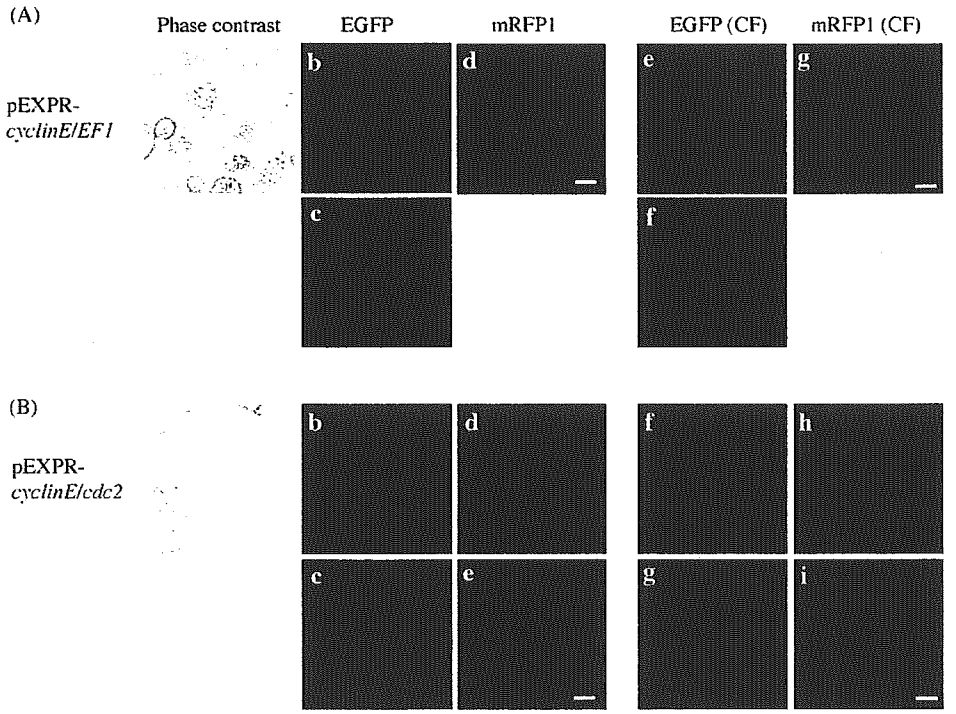

Fig. 2. Different expression levels of the *cpβ2*-cDNA and the *cpα1*-cDNA from a single Expression vector in transiently transformed cells. The Expression clones carrying both EGFP-tagged *cpβ2*-cDNA and mRFP1-tagged *cpα1*-cDNA in tandem on a single vector whose transcription is directed by the *cyclin E* and *EF-1α* promoters, respectively (A), or *cyclin E* and *cdc2* promoters, respectively (B), or either one of these fused cDNA (C and D) were used to transiently transform FRT-HeLa cells. The most left panels (A-a, B-a, C-a, C-d) show phase contrast, the other EGFP and mRFP1 images (A-b–d, B-b–e, C-b and c, C-e and f) were determined by fluorescence microscopy. The right side images (A-e–g, B-f–i, C-g and h) were generated using confocal laser microscopy. The images of A-c, A-f, B-c, B-e, B-g, B-i were enhanced images of those of A-b, A-e, B-b, B-d, B-f, B-h, respectively. The images shown in C-c and C-e were mock transfection. The white scale bars inserted in the images represent 10 μm. The other interpretations and conditions are as in Fig. 1 and the experimental procedures. In D, the expression levels of CPβ2-EGFP and mRFP1-CPα1 proteins produced from pEXPR-*cyclin E/EF1* clone (left) and pEXPR-*cyclin E/cdc2* clone (right) (pEXPR corresponding to A and B of Fig. 1, respectively) in the transiently transformed HeLa cells are shown. The relative fluorescent intensities measured were 7.6 and 100 for CPβ2-EGFP and mRFP1-CPα1 from pEXPR-*cyclin E/EF1* clone and 8.5 and 8.0 for those from pEXPR-*cyclin E/cdc2* clone, respectively. Shaded and closed bars represent the fluorescence intensities of EGFP and mRFP1, respectively.

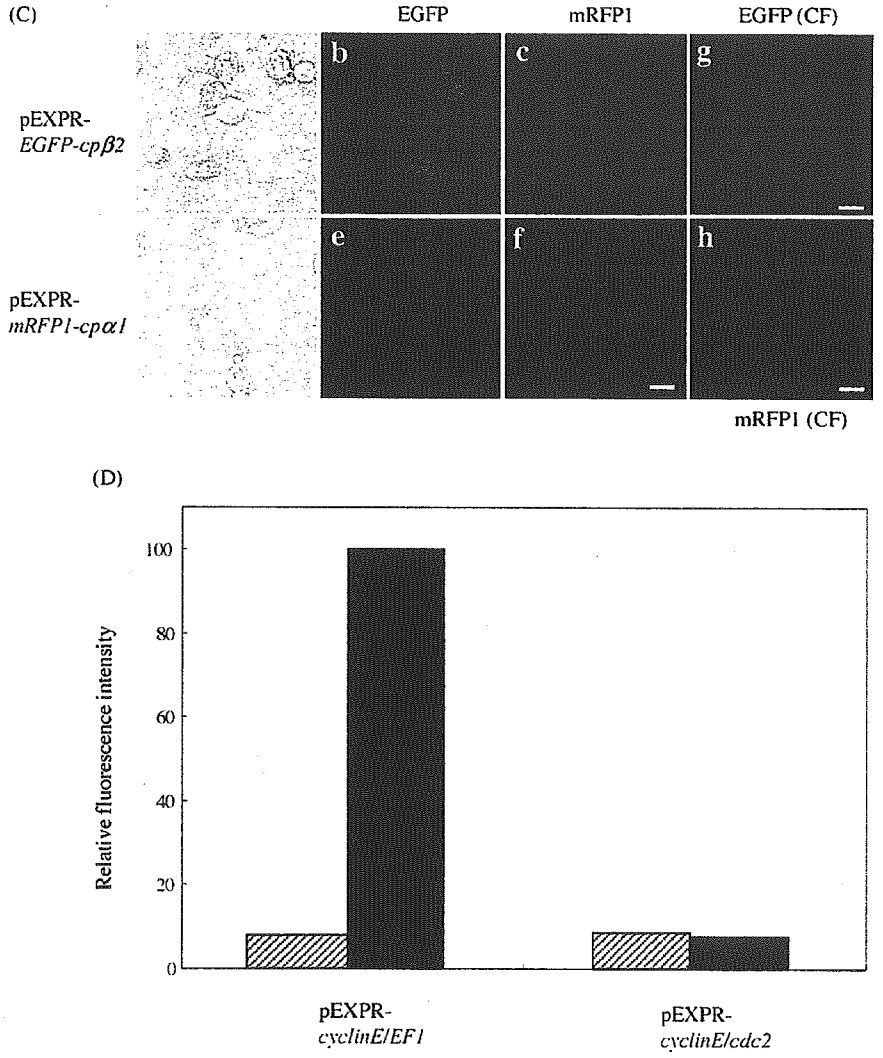

Fig. 2. (*Continued*).

3. Results

3.1. Promoters for transgene expression at near physiological levels in transformed cells

In eukaryotic cells, most of the intrinsic genomic genes are expressing in a cell-cycle dependent fashion. Use of the promoters, such as those prepared from *cyclin E*, *cdc2*, *cyclin B1* and *aurora A* genes of human genomic DNA which express at G1-S (Ohtani et al., 1995), S-G2-M (Furukawa et al., 1994), G2-M (Hwang et al., 1995) and G2-M (Tanaka et al., 2002) phases of cell-cycle division, respectively, would create testable transgene phenotypes in transformed cells by more closely mimicking the true physiological state. The molecular sizes of these signal DNA fragments prepared were 1091, 852, 248 and 1840 base pairs, respectively, including enhancer and transcription initiation sites. For comparison, the constitutively expressing, *EF-1α* (Kim et al., 1990) and CMV (Boshart et al., 1985) promoters were employed.

Relative transcriptional activities of these four different promoters were tested in comparison with *EF-1α* and CMV promoters, by using green fluores-

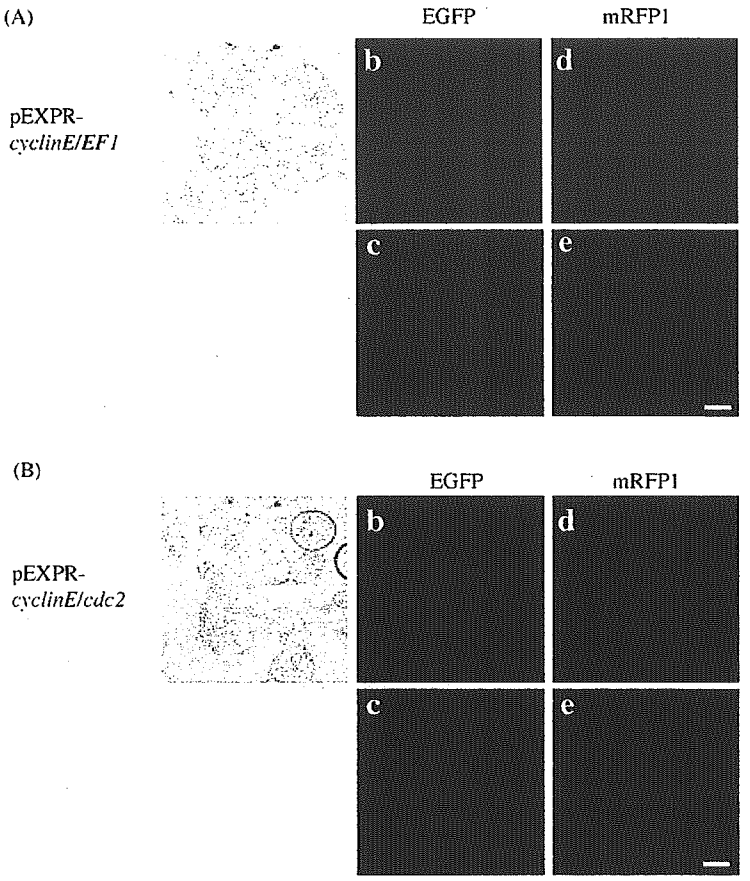

Fig. 3. Low-level expression of the *cpβ2*-cDNA and the *cpα1*-cDNA introduced simultaneously onto chromosomes in stably transformed cells. The expression levels of EGFP-tagged *cpβ2*-cDNA and mRFP1-tagged *cpα1*-cDNA on the pEXPR-*cyclin E/EF1* clone (A) and the levels of those fused cDNAs on the pEXPR-*cyclin E/cdc2* clone (B) are shown. Panels (A) and (B) show images of separated transformed cells from the colony of accumulated stable transformant HeLa cells. In A-c, A-e, B-c, B-e, the enhanced intensity images of A-b, A-d, B-b, B-d, respectively, are shown. The other interpretations and conditions are as in Fig. 1 and the experimental procedures.

cent protein, EGFP as a reporter gene (Cormack et al., 1996; Zhang et al., 1996). Six types of Expression clones, pEXPR-P*cyclin E-EGFP*, pEXPR-*Pcdc2-EGFP*, pEXPR-P*cyclin B1-EGFP*, pEXPR-P*aurora A-EGFP*, pEXPR-P*EF1α-EGFP* and pEXPR-P*CMV-EGFP* (Table 2) were constructed and used. By measuring the fluorescence emission intensity in transiently transformed HeLa cells, the relative activities for *cyclin E*, *cdc2*, *cyclin B1* and *aurora A* promoters were 3.9, 2.0, 1.0 and 1.3, respectively, compared to those of 24.1 and 338.0 for *EF-1α* and CMV promoters, respectively (data not shown). These human intrinsic promoters also exhibited significantly lower activity in other cell strains, such as 293 and mouse ES cells, compared to those of *EF-1α* and viral promoters (data not shown). Such promoters with 10 to 100-fold magnitude lower activity than conventional signals would be convenient for research of proteins synthesized from transgenes in the living cell.

3.2. Controllable production of two heterologous proteins from transgenes in transiently transformed cells

In contrast to conventional transfection procedures using mixed recombinant plasmid clones, use of a Multisite Gateway Expression clone carrying multiple cDNAs on a single vector has resulted in

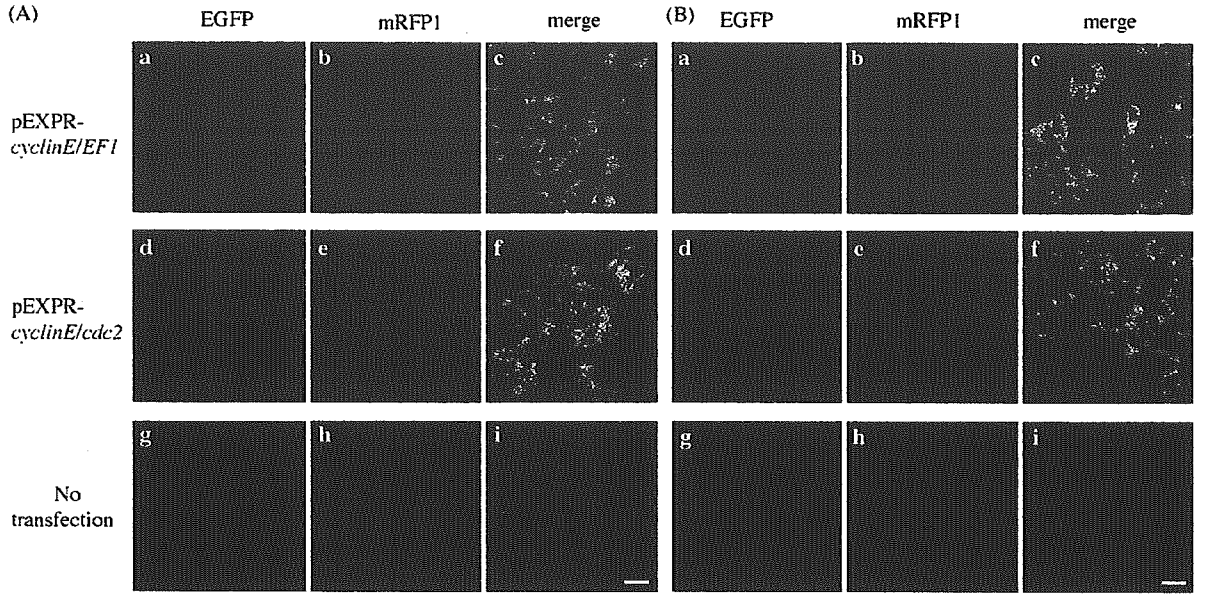

Fig. 4. Differential expression levels observed by confocal laser microscopy with two fluorescently tagged transgenes of *cpβ2* and *cpα1* introduced in the stably transformed cells. Stably transformed HeLa cells with the pEXPR-*cyclin E/EF1* clone (A-a–c) and with pEXPR-*cyclin E/cdc2* clone (A-d–f) are represented with the untransfected cells to show the auto-fluorescence of the cytoplasm of the cell as the control (A-g–i). The images obtained control experiments with the stably transformed Flp-In 293 cells are shown in (B). The emission intensity of EGFP measured by confocal laser microscopy was determined with 505–530 nm filter, followed by excitation by 488 nm (argon–krypton laser), and the emission intensity for mRFP1 was determined with 560 nm filter after excitation at 543 nm (helium–neon laser). The white scale bar indicates 20 μm (B). The other interpretations and conditions are as in Fig. 1 and the experimental procedures.

successful generation of transformant cells harboring these respective cDNAs at an equivalent number in each single cell (Sone et al., 2005). When two heterologous cDNAs were introduced into a cell at an equal copy number, the protein expression levels from the respective cDNAs depends principally on their promoter activities. In order to most closely reflect the physiological proteomic state in the cell during investigation of the intrinsic action and intracellular behavior of the target proteins, control of expression levels of the respective transgenes is important.

Two types of Multisite Gateway Expression clones harboring fused cDNA tandem structures were constructed (Fig. 1). The cDNA encoding *cpβ2* was C-terminally fused to the EGFP ORF and the cDNA encoding *cpα1*, was N-terminally fused to the mRFP1 ORF. The former fusion DNA was joined with *cyclin E* promoter and the latter fusion DNA was joined with *EF-1α* or *cdc2* promoter. The transiently transformed HeLa cells with either one of these Expression clones were observed to express both EGFP-tagged CPβ2 and mRFP1-tagged CPα1, thus ensuring that two different cDNAs were simultaneously present in the same cell.

As seen in Fig. 2A, all of the transformant cells expressed both CPβ2-EGFP and mRFP1-CPα1 at relative levels of approximately 1 and 10, respectively, by determination of fluorescent emission intensity of EGFP and mRFP1 (Fig. 2D). These values were consistent with the relative strengths of the *cyclin E* and *EF-1α* promoters (corrected for the approximate 1.6-fold higher emission intensity with mRFP1 over EGFP, data not shown). In Fig. 2B, a nearly equivalent level of expression with CPβ2-EGFP and mRFP1-CPα1 in the respective transformed cells is shown (see Fig. 2D). Considering the relative strength of the *cyclin E* and *cdc2* promoters (3.9 and 2.0, respectively), controllable expression of those two heterologous transgenes in a single cell to pre-determined levels was successfully achieved. For reference, expression levels with two respective *EF-1α* promoter-directed clones carrying a fused CPβ2-EGFP or mRFP1-CPα1 in the transformed cells are represented in Fig. 2C.

In Fig. 2, the results observed by using confocal laser microscopy are also represented with the fused cDNA tandem constructs together with the single cDNA constructs as control. The significance of these observations is described below.

3.3. Chromosomal integration of an expression clone with two heterologous cDNAs under different promoter control and stable expression in cells

Two types of expression plasmids for CPβ2-EGFP and mRFP1-CPα1, each of which carries a FRT recombination site, were constructed (Fig. 1). These plasmids can be integrated into a FRT site on chromosomal DNA by site-specific recombination mediated by Flp recombinase, generating a stable transformant cell. In these plasmids, expression of two cDNAs, *cpβ2* and *cpα1*, were controlled by the *cyclin E* and *EF-1α* promoter, respectively, or the *cyclin E* and *cdc2* promoter, respectively. The expression plasmid was introduced into HeLa cells harboring at least three FRT sites on the chromosomes (determined by Southern-blot analysis of the genomic DNA, data not shown). After positive selection of the transformed cells using hygromycin (see experimental procedures), the stable transformant clones were obtained.

As shown in Fig. 3A, the transformed cells bearing a plasmid carrying the *cyclin E/cpβ2* and the *EF-1α/cpα1* in tandem, expressed CPβ2-EGFP and mRFP1-CPα1 at a very low level whose fluorescent emission was barely visible using conventional microscopy (see also Fig. 2A). When the sensitivity of the microscopy was increased, each of separated stable transformant cells showed co-expression of CPβ2-EGFP and mRFP1-CPα1 at their respective pre-determined levels (Fig. 3A-c and A-e). Essentially similar observations were obtained with the transformant cell carrying transgenes of the *cyclin E/cpβ2* and the *cdc2/cpα1* in tandem (Fig. 3B). The fluorescent emission intensity of these separated cells was clearly more distinctive compared with the auto-fluorescence seen from cytoplasm (data not shown, see no transfection of Fig. 4).

Fig. 4 shows co-expression of CPβ2-EGFP and mRFP1-CPα1 in the stably transformed cells, observed by using the confocal laser microscopy. In these cells, fluorescent protein products were only localized in the cytoplasm but not in the nucleus. This remarkable feature was similarly observed with stable clones harboring a cassette of *cyclin E/cpβ2* and *EF-1α/cpα1* as well as another cassette containing *cyclin E/cpβ2* and *cdc2/cpα1*. Similar profiles of protein localization were also seen with the transiently transformed cells harboring a combination of tandem transgenes of *cyclin E/cpβ2* and *EF-1α/cpα1* and that of transgenes of *cyclin E/cpβ2* and *cdc2/cpα1* (Fig. 2A and B). These observations are consistent with the previous report that CPβ2 and CPα1 form heterodimers and localize to the cytoplasm, possibly being associated with actin fibers (Schafer et al., 1998). In fact, the dimer complex formation of CPβ2-EGFP and mRFP1-CPα1 proteins in the stable transformant cells was directly demonstrated by immuno–coprecipitation analysis using antibodies for EGFP and mRFP1 (Fig. 5).

4. Discussion

Introduction of multiple genes (cDNAs) simultaneously into cells using multigene-carrying plasmids ensures that all cDNAs are simultaneously present in the same cell in stoichiometric amounts (no gene dosage variation). In addition, control of transgene expression to achieve proper protein levels in the cell is desirable in order to obtain physiologically relevant information while investigating the intrinsic action of the intracellularly functioning proteins. Multisite Gateway technology offers a convenient vector platform for rapid construction of multi-cDNA expression plasmids useful for these purposes.

A conventional method for analysis of proteins labeled with bio-fluorphores (such as green fluorescent protein, GFP) in the cell has been to express a fairly large quantity of the protein produced from the transgene. This may affect cellular physiology and sometimes lead to non-physiological influences on protein function in the cell. We intended here to express cDNA and produce the protein at a relatively low level so as to not affect the intrinsic constitution and function of the intracellular proteome, while still allowing detection in a living cell.

In this report, two types of clones carrying fused cDNAs were employed. In these plasmids one cDNA fusion was transcribed from the *cyclin E* promoter and another from the *EF-1α* or *cdc2* promoter which produce CPβ2-EGFP and mRFP1-CPα1, respectively.